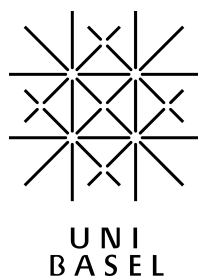

Thesis for the Completion of the Master's Degree in Nanosciences

Synthesis and Characterization of a Central Tripodal Subunit Enabling Dendritic Coverage of Gold Nanoparticles

ERICH HENRIK PETERS

March 2, 2015



Universität Basel
Group of Prof. Dr. M. Mayor



Acknowledgments

I would like to thank Prof. Dr. Marcel Mayor for granting me the honor of completing my master's thesis within his group here at the University of Basel and Prof. Dr. Thomas Pfohl who kindly agreed to be my co-referee. Special thanks goes to my supervisor Mario *loco* Lehmann for providing the molecular design, his outstanding support, his immense effort and patience in teaching me the ways of decent organic chemistry and for proofreading my thesis countless times as well as drawing the concept picture. I would also like to thank Viktor *loco* Hoffmann for creating a welcoming and entertaining atmosphere together with Mario throughout my entire time in Lab AC12, for his various inputs and his willingness to help in all kinds of situations. My gratitude goes to Gero Harzmann for kindly letting me use his bench, office and computer during his absence, to Dr. Loïc Le Pleux for proofreading parts of this work, Ina Bodoky who set my inventory account up, facilitating the completion of the experimental part and to Annika Büttner who made TGA even possible. Great thanks goes to Markus Gantenbein, whose ever-valuable advices rescued the proceeding of this work many times over, for sharing his expertise in organic chemistry whenever I had hit a seeming dead end. I would as well like to thank all the members of the Mayor group for allowing me to feel welcome. Further, my thank goes to Dr. Daniel Häussinger for allowing me to use the 400 MHz NMR spectrometer and Dr. Markus Dürrenberger and his team who granted us the access to one of their TEM.

Abstract

A novel tripodal central linking point enabling dendrimeric superstructures for the stabilization of Au NPs was proposed. In order to enhance the scope towards single-ligand coverage of the metal cluster, thioether-based oligomeric branch-like elongations were introduced. Au NP synthesis was successfully performed with three ligands (**Lig3-5**) as proven by NMR spectrometry, yielding small, monodisperse particles, as suggested by UV/Vis absorption spectroscopy and confirmed by TEM (**Au-Lig3**: 1.32 ± 0.37 nm, **Au-Lig4**: 1.14 ± 0.33 nm, **Au-Lig5**: 1.16 ± 0.29 nm). A correlation between side-chain length and stability was found, as well as between the number of solvation shell- and electronic repulsion-providing substituents and the particles' stability in organic solvents. TGA revealed a typical coverage of two ligands per particle in the case of **Au-Lig5** and a synthesis yield of 72 % with respect to gold.

The project will be continued towards ligands bearing longer side-chains as well as an electronically addressable functionalization as suggest our concept picture, enabling the reliable synthesis of solution-stable, small, monodisperse and monofunctionalized particles.



Contents

List of Abbreviations	iv
1 Introduction	1
1.1 Motivation	1
1.2 Physical Properties	2
1.3 Synthesis of Gold Nanoparticles	4
1.4 Influence of the Ligand Architecture	5
2 Project	6
2.1 Synthetic Strategy	7
3 Results and Discussion	9
3.1 Synthesis of the Ligand Core	9
3.1.1 Ligand Core Route A	9
3.1.2 Ligand Core Route B	11
3.1.3 Ligand Core Route C	13
3.2 Synthesis of the Oligomeric Branches	15
3.2.1 Branch A	15
3.2.2 Branch B	17
3.3 Synthesis and Characterization of the Gold Nanoparticles	18
3.3.1 Au NPs from Lig1 (Au-Lig1)	19
3.3.2 Au NPs from Lig2 (Au-Lig2)	20
3.3.3 Au NPs from Lig3 (Au-Lig3)	21
3.3.4 Au NPs from Lig4 (Au-Lig4)	24
3.3.5 Au NPs from Lig5 (Au-Lig5)	27
4 Conclusions and Outlook	30
5 Experimental	32
5.1 General Information	32
5.2 Synthetic Part	34
5.2.1 Synthetic Route A	34
5.2.2 Synthetic Route B	41
5.2.3 Synthetic Route C	46
5.2.4 Branch A	52
5.2.5 Branch B	57
5.2.6 Ligands	67
5.2.7 Gold Nanoparticles	72

List of Abbreviations

AIBN	2,2'-azo-bis(2-methylpropionitrile)
Au NP	gold nanoparticle
cat.	catalyst
DCM	dichloromethane
DMF	dimethyl formamide
DMSO	dimethylsulfoxide
eq	equivalent
EtOAc	ethyl acetate
EtOH	ethanol
GC/MS	gas phase chromatography and mass spectrometry
GPC	gel permeation chromatography
HOP	2-hydroxypropyl
<i>i</i> PrOH	isopropanol
LSPR	localized surface plasmon resonance
MALDI-TOF	Matrix-Assisted Laser Desorption/Ionization Time of Flight
MeOH	methanol
NBS	N-bromosuccinimide
NMR	nuclear magnetic resonance
OPE	oligo(phenylene ethynylene)
ppm	parts per million
quant.	quantitative
rpm	rotations per minute
RT	room temperature
TBME	<i>tert</i> -butyl methyl ether
TEM	transmission electron microscope
TGA	thermogravimetric analysis
THF	tetrahydrofuran
TIPS	triisopropylsilyl
TLC	thin layer chromatography
TMS	tetramethylsilane
TOAB	tetraoctylammoniumbromid
Trt	trityl
UV/Vis	ultraviolet and visible

1 Introduction

1.1 Motivation

Since several millennia, gold has been seen as a valuable material. Not only its shiny appearance, and its chemical inertia — both attributes desirable for the crafting of decorative objects or jewelry — have attracted common interest. Ever since the discovery of the astonishing optical properties of gold colloids (see figure 1¹) as staining agents for instance — as it is the case for the famous lycurgus cup — it is known that, scientifically speaking, more interesting attributes are to be found in this noble metal.

Only in the last decades, nevertheless, these unexpected properties have excited growing interest among chemists.



Fig. 1: Different colors of gold colloids of decreasing size.

First scientific reports about the synthesis of solution-stable gold colloids date from the mid 19th through the middle of the 20th century,¹⁻⁴ however, their popularity was not founded until the groundbreaking works by Turkevich *et al.*⁵ on water-soluble gold colloids, establishing today's referential route to stabilize colloidal gold by reduction of chloroauric acid by citrate, which at the same time acts as the stabilizing ligand. Further works with various approaches followed,⁶⁻⁸ but it was not until the discovery of the pathbreaking Brust-Schiffrin two-phase method^{9,10} (see also section 1.3) that ligands based on thiols unfolded their popularity in this field of research. The advantages thiol ligands are given by their outstanding durability upon stabilization of gold clusters, their excellent binding ability to gold, as well as their uncomplicated handling common organic solvents after precipitation, and to be easily chromatographed without alteration of their properties.^{9,10}

A broad variety of applications of noble metal colloids have been implemented. In medicine, for instance, gold nanoparticles have been used in the treatment of rheumatic arthritis⁶ for years or have proven to be promising and reliable sensors in the detection of lung cancer¹¹ or other biological markers¹²⁻¹⁵ and were investigated in their ability to selectively destroy breast cancer cells¹⁶ or to offer a promising route for selective delivery of cancer treatment drugs.^{16,17} Potential technical applications comprise (opto-)electronic devices¹⁸⁻²⁴ by exploiting their size-dependent properties as single quantum dots or ensemble of carefully arranged quantum dots²⁴⁻²⁸ as the implementation of gold colloids in efficient catalysis of a broad multitude of chemical

¹image source: <http://chemistry.uchicago.edu/faculty/faculty/person/member/philippe-guyot-sionnest.html>, as of Feb 7, 2015

reactions^{29–31} or in optical as well as thermal sensing.²⁴

In this work, we report the full synthesis as well as the properties of five novel tripodal thioether-based ligands with oligomeric elongations enabling three-armed chain-like molecule design (**Lig1-5**; see scheme 1 on page 6) to stabilize Au NPs. We also report the ligands’ ability to stabilize Au NPs upon synthesis as stated in the *Brust-Schiffrin* protocol. Furthermore, we characterize the stable particles by UV/Vis absorption spectroscopy, followed by NMR and TGA as well as their size distribution by TEM.

This work is seen as a continuation of previous investigations on functionalized thiol- and thioether-based ligands by Peterle *et al.*,^{32,33} Hermes *et al.*^{34–36} and Lehmann *et al.*ⁱⁱ Our motivation is given by earlier reports that proved tripodal thiol ligands to be more efficient in attaching to gold surfaces as well as in stabilizing gold colloids than their monopodal or even dipodal counterparts,^{29,37–43} and by earlier published syntheses of Au NPs stabilized by only one ligand enabling monofunctionalization through introduction of a OPE group at the central linking point.^{36,44}

1.2 Physical Properties

The exotic properties of Au NPs arise from their small size. As they consist of a small number of gold atoms only, they can be approached as a quantum well with finitely high potential walls,^{12,15,26,27} thus they lose their typical bulk behavior, and rather obey to the laws of quantum mechanics when the particle size is in the range of the de Broglie wavelength of their conducting electrons.⁴⁵ If this is the case, the energetic states of the confined electrons lose their metallic band structure,²⁷ and split up to discrete levels as described in the quantum well model^{12,26} (see fig. 2). They are therefore often referred to as *big*,⁴⁵ *artificial*³⁵ or *super*⁴⁶ atoms.

With increasing size, the sharp electronic states start broadening, until a metal-like band structure is observed.⁴⁵ The particle-bulk transition has been found to be in the vicinity of 1-2 nm.^{25,45}

The quantum dot behavior offers a high versatility for the implementation of Au NPs as

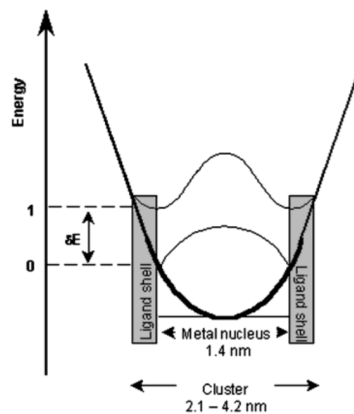


Fig. 2: Quantum well approach to a metallic NP. The diameter of the particle corresponds to the width of the quantum well. The ground state and first excited state are drawn in the quantum well.²⁶

ⁱⁱmanuscript in preparation

building blocks of electronic quantum devices,^{12, 18, 19, 22, 24, 26} as nanotransistors.⁴⁵ Also, low-dimensional arrays of Au NPs for their implementation in electronic circuits have been investigated. One of the major challenge herein is to arrange the particles such that the collective of the electron wave functions interacts constructively.²⁸ In order to overcome these demands, cautiously tailored matrices for the self-assembly of NP superstructure²⁴ as well as tailor-made chemical spacers made from rigid oligo(phenylene ethynylene) (OPE)-rods^{32, 35} as functional units have been investigated. A scheme showing the influence of spacial arrangement is shown in figure 3.

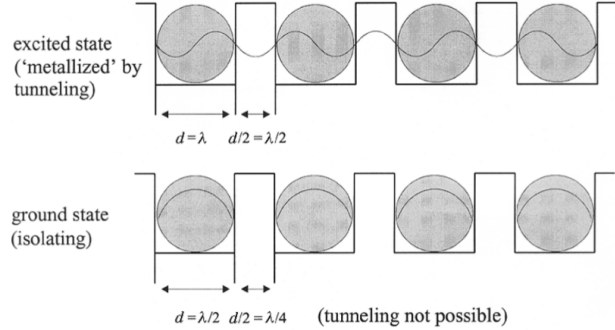


Fig. 3: Schematic representation of the interference between the collective of the NP electron wave function. Above: in the first excited state, all wave functions can interfere constructively; the NPs act as metal. Below: at ground state, all wave functions interact destructively; the NPs behave as insulators.²⁶

In contrast to other metal NPs, Au NPs made from 55 gold atoms (Au₅₅; also known as *Schmid's cluster*) have proven to work as single-electron switches at room temperature due to their unusual Coulomb blockade at such comparably high temperatures.⁴⁵

Similarly interesting properties of metal — and particularly gold — NPs in general are given by their unusual optical spectra that originate from the very same quantum

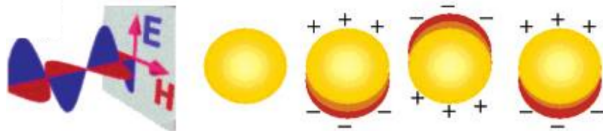


Fig. 4: Schematic representation of the interaction between the electric field of incident light and a spherical NP. The electron cloud is moved from its initial location, creating an oscillation in phase with the electric field of the incoming light.⁴⁷

effects as their electronic characteristics.²⁷ Upon interaction with the incident light, the collective valence electrons of the NPs oscillate along with the light's electric field, creating a restoring force (see figure 4). This effect is known as LSPR as described by the Mie theory.^{27, 48, 49} LSPR only occurs if the wavelength of the incident light matches the frequency of the LSPR, and is therefore strongly size-dependent as with increasing size, a red-shift of the LSPR is observed^{12, 15, 50} which explains why solutions with smaller particles have a red color, while solutions with bigger particles are blue (see figures 1 and 5). Unlike other metals, NPs made from gold, silver and copper exhibit their LSPR in the visible light range due to their d-d band transitions,^{47, 50} which is not observed for any other metal.

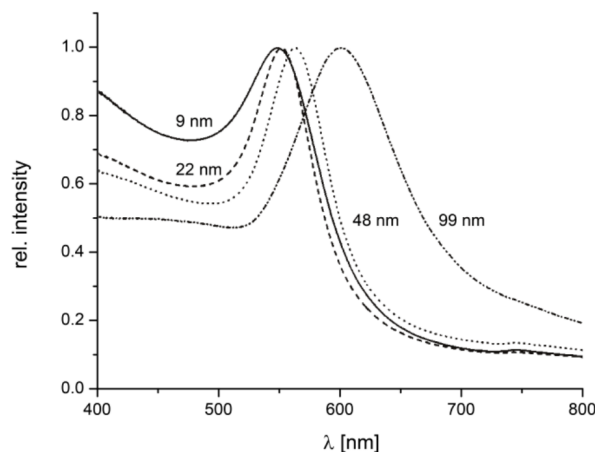


Fig. 5: Size-dependence of UV-Vis absorption of gold colloids in water. The bigger the diameter, the more the LSPR peak is red-shifted.⁵⁰

1.3 Synthesis of Gold Nanoparticles

At this place, it is important to point out that since this work will present and discuss the approach to the Brust-Schiffrin two-phase method for the synthesis of Au NPs, only this very procedure will be explained in this section.

Based on the methods used by Faraday,¹ Brust and Schiffrin proposed the reduction of aqueous gold salt in an organic solvent and stabilization of the growing gold clusters upon addition of thiol ligands.⁹

Aqueous chloroauric acid is transferred to the organic phase by a phase-transfer catalyst. In this case, TOAB dissolved in DCM is the catalyst of choice. Reduction of the gold salt by sodium borohydride in the presence of an appropriate ligand allows the surface reaction to take place during nucleation and particle growth, delivering highly monodisperse particles.^{9,10}

The size and stability of the particles, however, is strongly dependent on the ligand. Bulk, steric hindrance, flexibility and number of binding sites of the ligand all have an influence of the binding and stabilizing properties and have been reported in numerous occasions.^{37,38,40,43,51–54}

As mentioned above, in this work, we discuss not only the ability of tridentate thioethers to stabilize Au NPs, but also three-armed chain-like derivatives of these tridentate precursors that stabilize Au cores by their thioether moieties. First works with thioethers have proven their ability to stabilize Au NPs, despite their weaker sulfur-gold interactions compared to thiols. The resulting particles were, however, bigger in size and less stable upon heating.⁵⁵

Further research in oligomeric and dendrimeric ligands delivered thioether-based ligands stabilizing Au clusters with similar size and thermal stability as thiols,^{32–35,44} bearing the major advantage of size tunability due to size-dependence on the oligomer chain length. Furthermore, these studies revealed that thioether-gold bonds have scope for self-correction in the ligand-

gold complexation with the sulfur in the thioether moieties able to distribute themselves on the particle surface via quasi-reversible S-Au bonds, so to obtain favorable ligand conformation.

1.4 Influence of the Ligand Architecture

In previous reports,^{32,ii} the influence of the ligand shell thickness to NP core size ratio on the solubility as well as the importance of the gap between two sulfur atoms within one ligand has

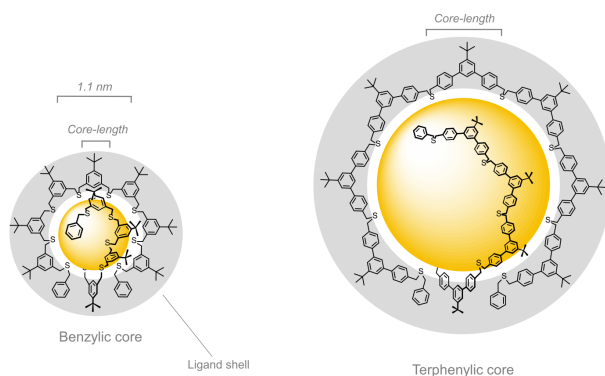


Fig. 6: Schematic representation of the ligand shell. Left: ligand as proposed by Peterle et al.³³ Right: ligand as proposed by Lehmann et al.ⁱⁱ While the particle on the left hand side is very well soluble, due to its thick ligand shell in comparison with the Au core size, while the particle on the right hand side proved to be insoluble and showed tendencies to form Au agglomerates, as the ligand shell is rather thin and the space between the individual sulfur atoms of the ligand is much larger than for the ligand on the left side.

been investigated and discussed. It has been found that, in order to provide enough steric repulsion — or electrostatic respectively — the ligand shell thickness has to match distance between the individual sulfur atoms within the ligand. Further, the ligand has to provide its own solvation shell by introduction of e.g. *tert*-butylic groups.⁵⁶ Also, the angle formed between the two neighboring sulfur sites and the center of the gold core (*biting angle*) plays a significant role, as it decides upon the conformation of the ligand core and thus its energetic favorability, as well as the density of the ligand coverage of the gold cluster. Furthermore, we postulate that the particles size is strongly dependent, not only on the size of the ligand and its number of S-Au binding sites, but also on the biting angle. A direct correlation between metal core size and bidding angle has, nevertheless, yet to be proven and is subject to current research. Figure 6 shows a scheme explaining the influence of the ligand architecture.

been investigated and discussed.

It has been found that, in order to provide enough steric repulsion — or electrostatic respectively — the ligand shell thickness has to match distance between the individual sulfur atoms within the ligand. Further, the ligand has to provide its own solvation shell by introduction of e.g. *tert*-butylic groups.⁵⁶ Also, the angle formed between the two neighboring sulfur sites and the center of the gold core (*biting angle*) plays a significant role, as it decides upon

2 Project

In contrast to above stated earlier studies, we propose the — to our knowledge very first — synthesis of a series of unfunctionalized tripodal benzylic thioether ligands with a tetraphenylmethane core (see figure 7). Very similar, OPE-functionalized ligands have thoroughly been investigated on their adsorption characteristics upon binding on Au surfaces in the past decade,^{57–60} and will be targeted as continuation of this project. No reports about their ability to stabilize Au NPs have, however, not been reported so far.

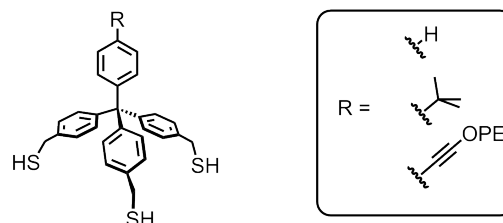
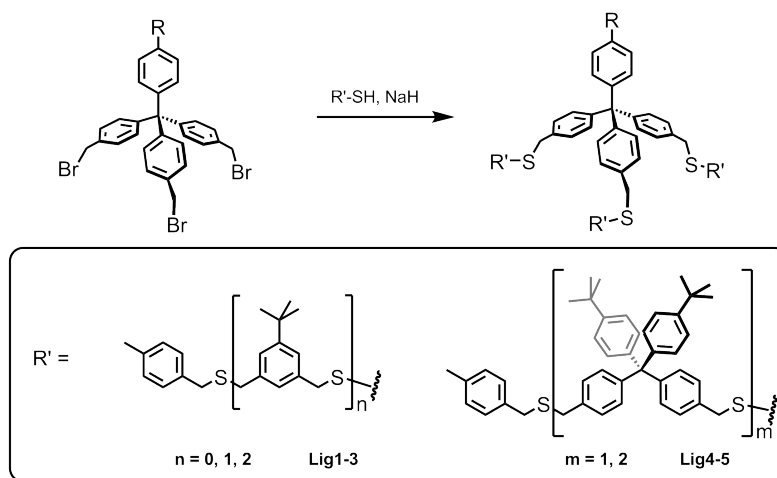


Fig. 7: First ligand proposal. This work reports the synthesis towards unfunctionalized target compound with $R = H$.

We also propose the introduction of thioether-based oligomeric chain-like elongations at each thiol site towards dendrimeric superstructures in order to increase the solubility of the particles as well as their size in dependence of the oligomeric chain length and biting angle, as can be seen in scheme 1.

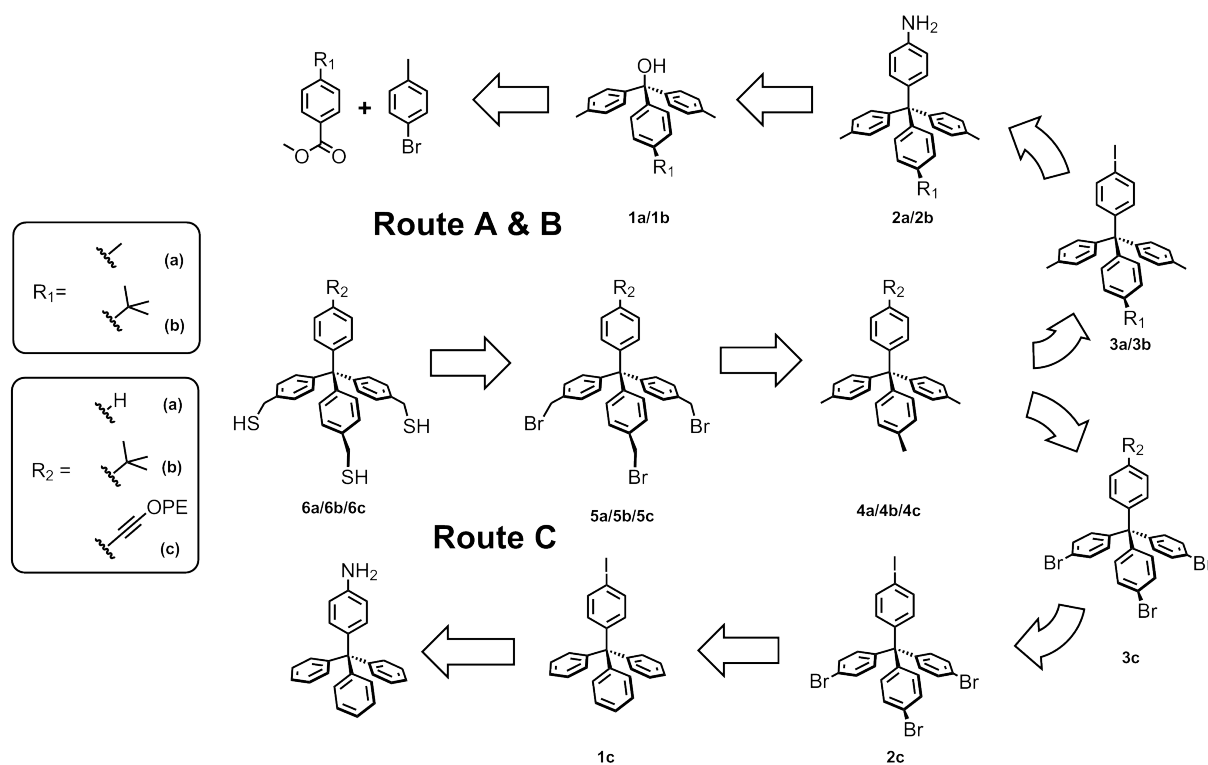


Scheme 1: Chain-like elongations enabling three-armed oligomers. In this work: $R = H$.

The synthesized ligands were used for the synthesis of Au NPs, following the Brust-Schiffrin protocol. The resulting particles were characterized by UV/Vis-absorption, NMR, TGA as well as TEM, and are also part of this report.

2.1 Synthetic Strategy

Two possible synthesis pathways were identified from an initial retrosynthetic analysis as can be found in scheme 2. The synthesis of the tetraphenylmethane core structure from an initial *Grignard* reaction and subsequent electrophilic aromatic substitution, followed by iodination was found, leading to compound **3a** that offers a high versatility thanks to its iodine in para-position,

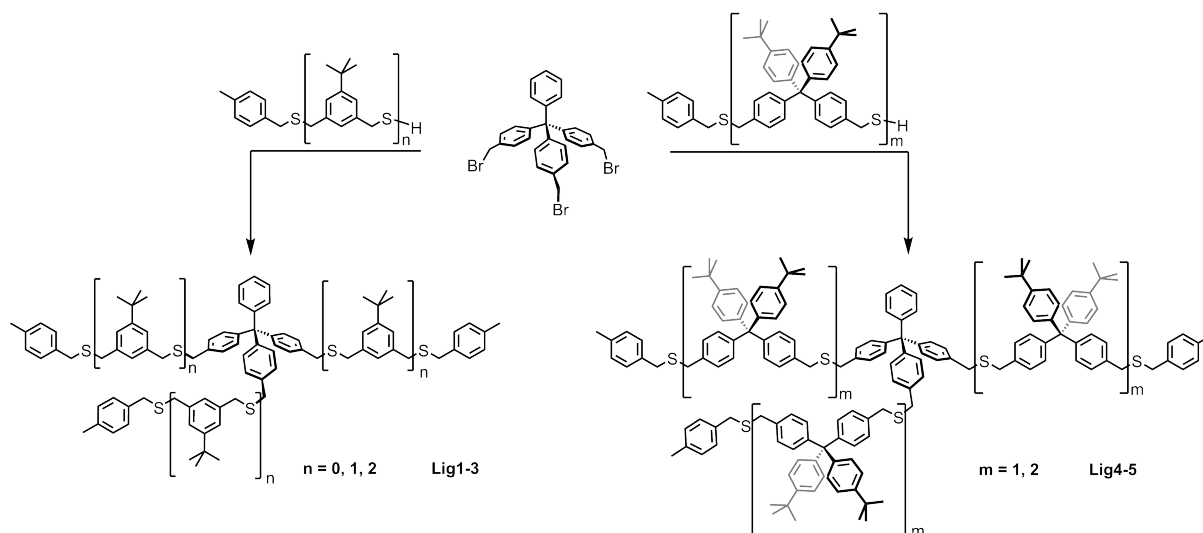


Scheme 2: Retrosynthesis of the target molecules.

and thus the possibility of introducing a functional moiety, allowing electronic addressing at this same site. On the other hand, the second proposed pathway bears the tetraphenyl methane core from the very beginning on, as it starts with tritylaniline. Over *Sandmeyer*-type iodination and subsequent benzylic bromination, this way leads to the selectively functionalizable iodo-tribromo-compound **2c**. After functionalization and methyl-halogen-exchange, the synthesis follows the same pathway as stated in the first proposal. We chose this two-way approach in order to investigate on the feasibility as well as the efficiency of both ways compared to one another.

Throughout the duration of this work, we have investigated one additional synthetic pathway in order to introduce a *tert*-butylic group to the central tripodal unit. We compared both: the introduction in a later step, as well as its introduction in the very first step by *Grignard* reaction. The completed central linking point bearing said *tert*-butylic group has, nevertheless, not yet been completed and is subject of further research.

After finding that the thiolated tripodal compound **6a** was insoluble in any solvent whatsoever (see discussion), we decided use the tribromo precursor as a central linking point for the introduction of two different oligomeric elongations, introduced to the central tetraphenyl core by S_N2 reactions, and attached by thioethers. For both oligomeric elongations, we chose a stepwise oligomerization procedure that had already been established in this group,^{33,ii} and are shown in scheme 3.



Scheme 3: Oligomeric elongations introduced by S_N2 reaction.

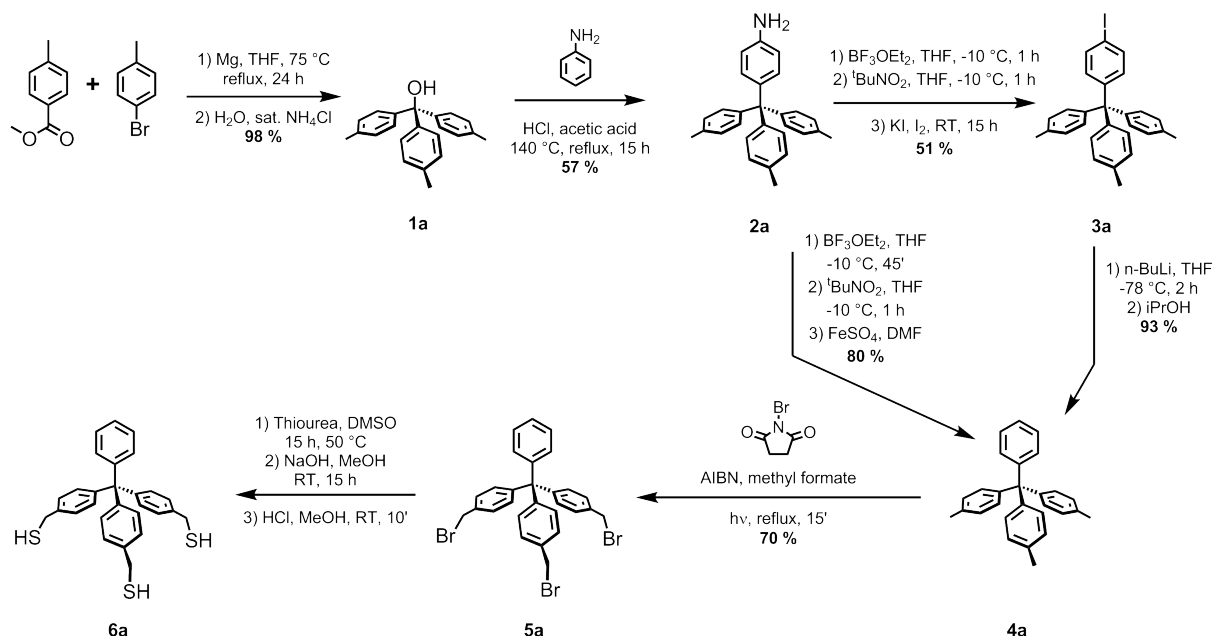
For the sake of convenience, these oligomeric elongations will be called *branches* from this point forward.

ⁱⁱLehmann et al. manuscript in preparation

3 Results and Discussion

3.1 Synthesis of the Ligand Core

3.1.1 Ligand Core Route A



Scheme 4: Overview of the synthesis to trithiol **6a** (route A).

Precursor **1a** was obtained quantitatively from a twofold *Grignard* reaction on the ester precursor with 4-bromotoluene. Subsequent electrophilic aromatic substitution with aniline gave the tetraphenyl methane core in moderate yield. A one-pot *Sandmeyer*-type reaction delivered the substitution of the amine by iodine through preliminary *in situ* formation of its diazonium salt. The rather low yield of merely 51 % suggests a need to optimize this synthesis step, for the main side product consists of the unfunctionalized compound **4a** which is likely to be favored if during the formation of the diazonium salt the temperature of the mixture highly exceeds 0 °C, leading to its defunctionalization. This suggests that more reliable temperature control would be necessary in order to improve the yield. Further, it is important to let the mixture stir for long enough before adding the iodine and the potassium iodide so all starting material can form the diazonium salt. Also, even slower warming after addition of said two reactants should allow less diazonium salt to be decomposed in the undesired manner, defunctionalizing the tetraphenyl core. The much more efficient defunctionalization of **2a** towards **4a**, which follows a very similar procedure, supports the above stated findings.

Compound **3a** can be seen as a versatile starting material for the introduction of functional groups — electronically easily addressable units as OPE rods, for instance — at the iodo-site of the molecule. In order to proceed to the non-functionalized trithiol **6a**, the amine was

defunctionalized by formation of the diazonium salt and subsequent defunctionalization in a solution of FeSO_4 in DMF. An alternative path to proceed to the defunctionalized precursor **4a** was to perform a lithium-halogen exchange via *n*-BuLi on **3a**, followed by protonation by *i*PrOH.

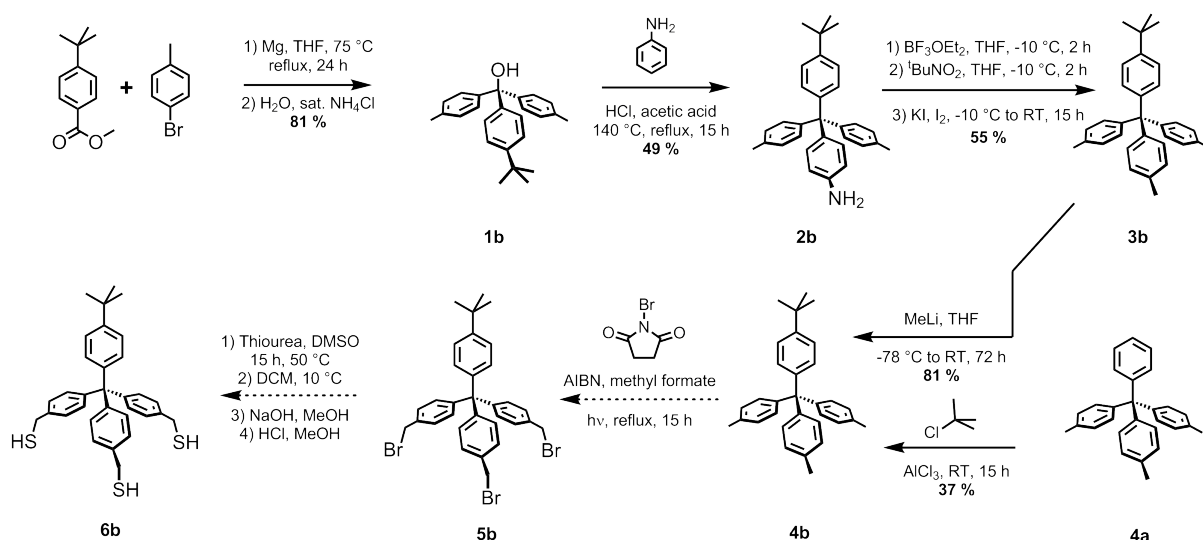
The benzylic tribromide **5a** was obtained by radical reaction upon illumination with a halogen lamp with NBS as bromine source and AIBN as radical initiator. This reaction proved to be very fast and efficient in comparison with similar reaction performed in former studies.ⁱⁱ Its purification from the respective mono- and dibromides, however, turned out to be rather difficult. This was due to (1) their poor solubility in common organic solvents and (2) they were virtually impossible to separate by column chromatography. We chose a recrystallization procedure in several steps as proposed by Tian *et al.*⁶¹ from hot chloroform.

In order to substitute the bromine by a terminal thiol, the tribromide was treated with excess of thiourea in DMSO to form its thiuronium salt within 15 hours, which could then easily be precipitated and filtered off by addition of DCM. The salt was then redissolved in MeOH and hydrolyzed with degassed aqueous 1 M NaOH. Immediate precipitation of the trithiol **6a** was observed upon acidic workup with aqueous 1 M HCl. Further work with this template ligand as well as its analysis was rendered impossible by its outmost insolubility in organic solvents. We believe that these solubility issues arise from the formed cage through two tetrahedral precursors via hydrogen bridges between the respective sulfhydryl head groups. For this reason, we decided to introduce branch-like oligomeric elongations to **5a** at its benzylic Br-ends via $\text{S}_{\text{N}}2$ reaction to overcome the solution issues encountered for **6a**. The synthesis of the branches as well as the follow-up synthesis towards **Lig1-5** will be discussed in section 3.2.

We have not yet performed studies in the stabilization behavior of OPE-functionalized ligand centers such as **6c**. Evidence that tridentate thiols are very reliable ligands for Au NPs has been presented several times in earlier works.^{37,38,40,43} Furthermore, OPE-functionalized compounds similar to **6c** have been reported as readily soluble.⁵⁸ For this reason, further research should include the synthesis of OPE-functionalized trithiol **6c** as well as studies on its ability to stabilize Au NPs.

ⁱⁱLehmann et al. manuscript in preparation

3.1.2 Ligand Core Route B



Scheme 5: Overview of the synthesis to trithiol **6b** (route B). The dashed arrows represent not yet performed reactions.

Similarly to *route A*, in this second pathway, the tetraphenyl methane core of ligand **6b** was obtained from a twofold *Grignard* reaction — in significantly lower yield in comparison to *route A* — followed by a subsequent electrophilic aromatic substitution to an aniline. Substitution of the amine by a *Sandmeyer*-type reaction provided the precursor **3b**, for which we encountered the very same issues as previously discussed for the same step in *route A*. The third methylic group towards **6b** was introduced by lithium-halogen exchange and immediate nucleophilic attack by the methyl anion.

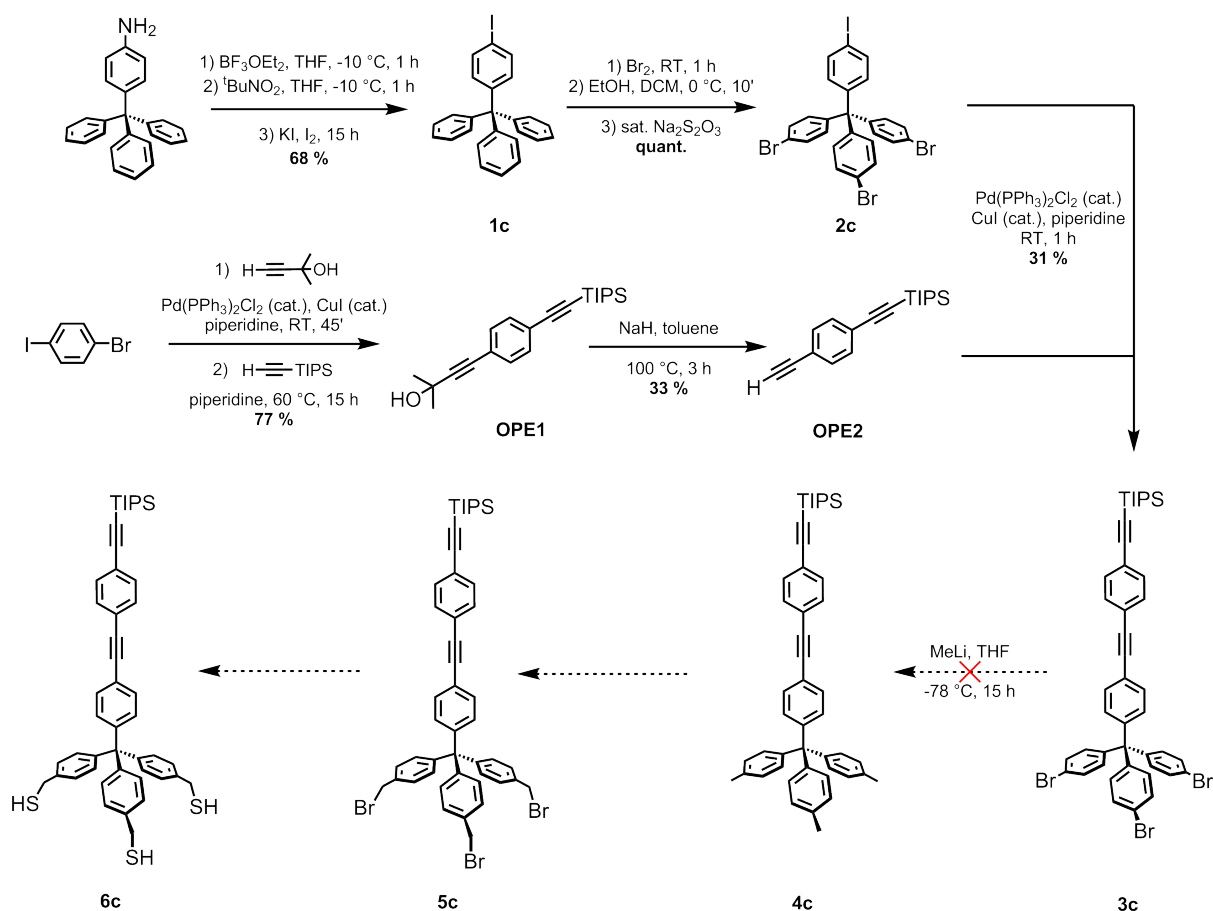
Compound **4b** can also be obtained by *Friedel-Crafts* alkylation on compound **4a**, using AlCl_3 as a catalyst. In the here reported reactions, however, the *Friedel-Crafts* alkylation worked with surprisingly and atypically low yield of 37 %. Three spots were visible by TLC: starting material, *p*-monosubstituted, and *m*-disubstituted; all purifiable by automated GPC with similar yields. Even stirring the reaction for longer time or using smaller amounts of reactant did not change this finding. Although if *m*-disubstitution was found to be favorable, we could not isolate any *m*-monosubstituted compound. Also, $^1\text{H-NMR}$ spectra of the side product identified as monosubstituted by GC-MS showed no *m*-monosubstituted impurities in the *p*-monosubstituted compound. This step requires more attention, as for instance, the influence of the catalyst have been thoroughly investigated as well as reported;⁶² and should be taken into consideration during the continuation of this project.

At this point, it has to be pointed out that both ways proposed in this work towards precursor **4b** — from *route A* over *Friedel-Crafts*-alkylation of **4a** as well as from *route B* — have an overall

yield of 17 % from the first synthesis step to compound **4b**. Since *route B* requires one step less, one might think that this route would be the one to chose, but we strongly recommend to start from *route A* towards the *tert*-butyl-functionalized trithiol **6b**, since *route A* proves to be more versatile when it comes to functionalization.

The further route towards trithiol **6b** has not been completed to date, and is still under investigation. We expect to find that the *tert*-butylic group in *para* position of the central phenyl might help overcoming the solubility issues encountered with target compound **6a**, since several works reported the solubility in common solvents of halogen-functionalized derivates of the same compound.^{57,60} Furthermore, we may expect compound **6b** to be more efficient in stabilizing Au NPs than soluble derivates of **6a** such as **Lig1** or **Lig2** due to stronger S-Au bonds from thiols than from thioethers.⁵⁵ We suspect that non-branched ligands might, however, result in significantly less control over the size distribution of the resulting Au NPs, although the number of dentation has been reported to be essential for the size of the stabilized particle cores, since the curvature of the metal core surface is tightly connected to the number of dentation and the rigidity of the ligands.^{28,37,43} These previously reported studies were performed with more rigid ligands than the here proposed trithiol **6b** due to shorter distance from the sulfhydryl head groups to the ligand core, which, as we believe, allows a larger tolerance towards variation in the particle curvature, or in other words: the particle size.

3.1.3 Ligand Core Route C



Scheme 6: Overview of the synthesis to trithiol **6c** (route C).

This pathway was proposed as an alternative to *route A* and *B*, starting from commercially available tritylaniline, following a similar route to the works of Hutchison *et al.*⁶³ A *Sandmeyer*-type reaction provided substitution of the amine by iodine in good yield, but still leaving space for improvement as discussed above. Subsequent dissolving in pure bromine and work-up with aqueous sodium thiosulfate and DCM afforded monoiodo-tribromo compound **2c**. *Sonogashira* coupling with the previously synthesized OPE-rod delivered the functionalized tetraphenyl methane core of precursor **3c**. The considerably low yield of 31 % is due to homo-coupling of the free acetylenes of the OPE-rod; a well-known side reaction mediated by the copper cocatalyst in presence of oxygen.^{64,65} In order to overcome these efficiency issues, it is imperative to degas the reaction mixture for longer time, or to use a copper-free *Sonogashira*-type protocol.⁶⁶ Methylation of the phenylic bromines by MeLi gave no conversion. Only decomposition of the starting material was observed, showing that *route C* towards the trithiolic central linking point leads to a dead end, and had therefore to be given up.

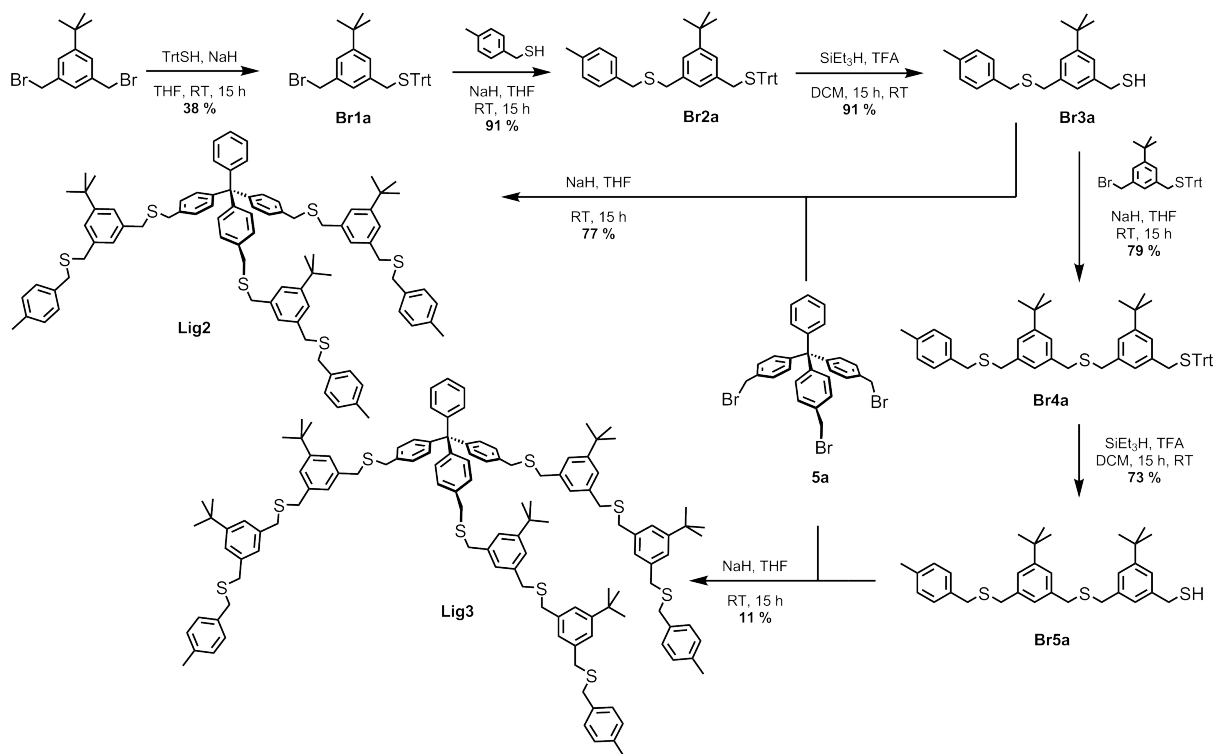
The proposed OPE-rod was synthesized by *Sonogashira* coupling of HOP, and TIPS-protected

acetylene to 1-iodo-4-bromo benzene and subsequent deprotection of the HOP-protected site with NaH, delivering the free acetylene for a final *Sonogashira*-coupling to a core-precursor in 33 % yield. This considerably low yield was due the free acetylene's strong tendency to undergo homo-coupling, although the glassware was thoroughly washed with sulfuric acid beforehand to remove any residue of homo-coupling mediating copper species. In order to achieve higher efficiency, the HOP-deprotection can also be performed by treatment with stoichiometric amounts of KOH and K₃PO₄ instead of NaH.⁶⁸

The completion of this synthesis route — which should be one of the major aims in the continuation of this work — can, nevertheless, still be performed by *Sonogashira* coupling of the proposed OPE-rod to a *p*-iodo-derivative of **6a**. In order to achieve this, compound **3a** can be used as a starting material for benzylic bromination, subsequent benzylic thiolation, followed by *Sonogashira* coupling.

3.2 Synthesis of the Oligomeric Branches

3.2.1 Branch A



Scheme 7: Overview of the branch synthesis to **Lig2-3** (branch A).

The synthesis of *branch A* was started from 1,3-dibromomethyl-5-*tert*-butylbenzene. In order to prevent polymerization, we chose to statistically protect one benzylic site by tritylthiol upon treatment with sodium hydride to obtain **Br1a**, followed by endcapping at the remaining benzylic site by similar introduction of *p*-tolylmercaptane. Deprotection, and thus formation of the free thiol, was performed by treatment with trifluoric acid in presence of triethylsilane, acting as a cation scavenger. Similar to the protection and the end-capping steps, the mono-endcapped branch **Br3a** was attached to the tribromo compound **5a** via S_N2 reaction in presence of sodium hydride, giving ligand **Lig2** as a target compound in 77 % yield.

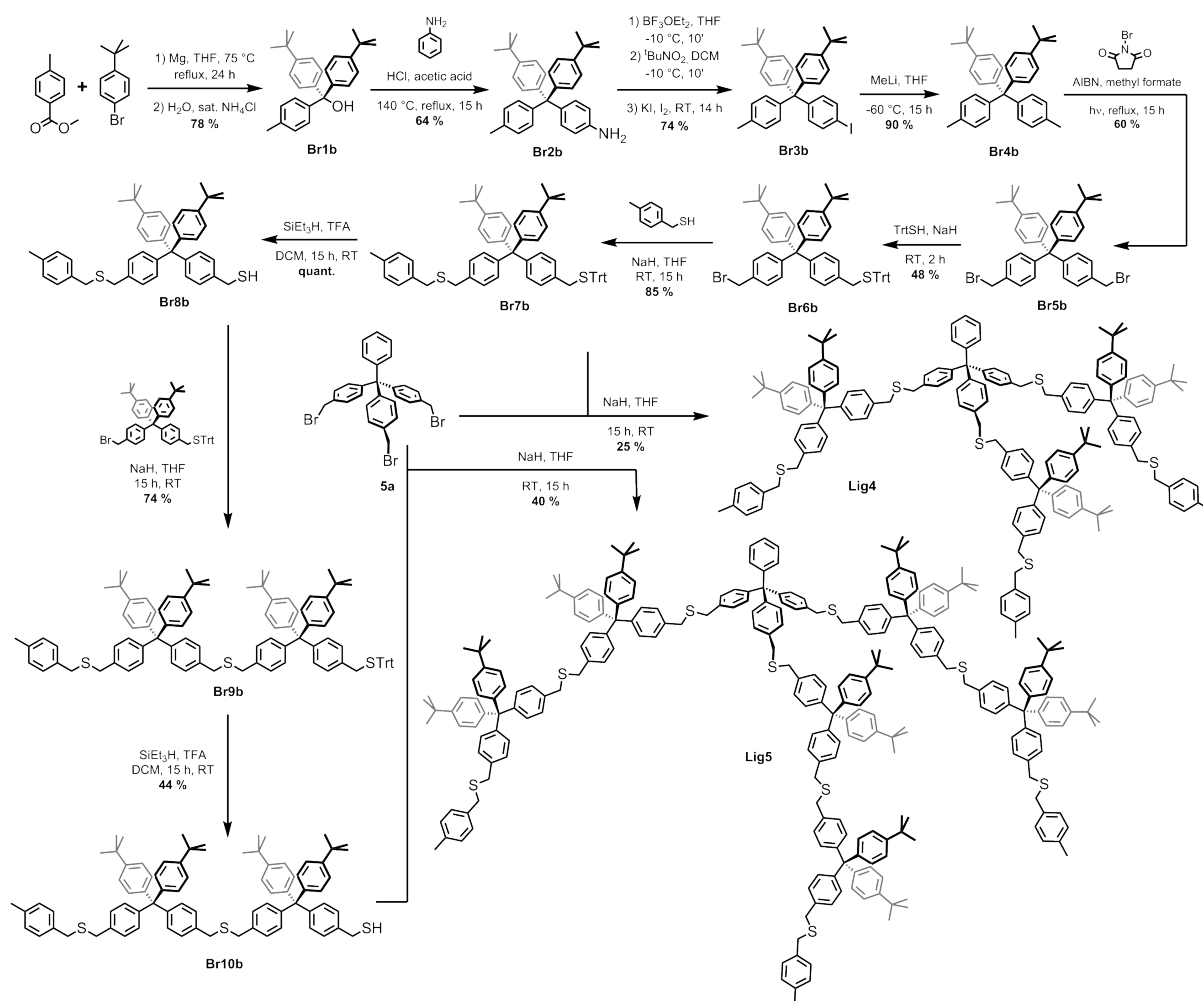
Thiol **Br3a** was as well used as a starting material for the oligomerization towards longer branches, using an elongation-deprotection strategy as developed by Peterle *et al.*³³ The free thiol was used for elongation of *branch A* by S_N2 reaction with the monoprotected precursor **Br1a**, furnishing the dimeric precursor **Br4a**, which was deprotected as stated above to obtain the dimeric thiol **Br5a** in 73 % yield. Nucleophilic substitution with compound **5a** delivered ligand **Lig3** in surprisingly low yield, despite rigorous degassing of the solution by a steady argon stream for 15 minutes to prevent the formation of disulfides, and although TLC control showed full conversion of **5a**, and only two new spots: ligand **Lig3** and much likely twofold substituted

ligand.

Similar issues have been reported by Peterle *et al.*³³ while trying to attach similar oligomeric chains to a central OPE-functionalized linking point by the very same reaction conditions. As a solution to this issue, they proposed to use the thiolated central unit as a starting point for the stepwise oligomerization of the side chains, followed by subsequent functionalization of the central unit. In the case described here, this approach seems rather inconvenient due to the low solubility of **6a**. It is, however, known that a similar trithiol, functionalized with iodine in *p*-position of the free benzene, is well soluble in common solvents.^{57,60} For this reason, we foresee to proceed this project from compound **3a** towards the synthesis of a trithiolated central linking point bearing a free iodine accessible for further functionalization, as well as free thiols that enable easy stepwise side chain growth for the synthesis of bigger and more complex dendrimers in a more efficient manner.

In general, the oligomerization procedure can be repeated *ad voluntatem* if need be.

3.2.2 Branch B



Scheme 8: Overview of the branch synthesis to **Lig4-5** (branch B).

As a second step towards oligomeric dendrimer-like structures, the introduction of the bulky tetraphenyl methane core ligand as proposed by Lehmann *et al.*ⁱⁱ was chosen. The general synthesis route is very similar to the synthesis route to trithiolic ligand **Lig1**.

The tetraphenyl methane core was synthesized by a twofold *Grignard* reaction, followed by electrophilic aromatic substitution with aniline in good yield towards branch precursor **Br2b**. Substitution of the amine by iodine through a *Sandmeyer*-type procedure, and subsequent methylation with MeLi delivered compound **Br4b** to which radical benzylic bromination as discussed for ligand core *route A* and *B* was performed. In order to synthesize branch **Br8b**, the very same monoprotection-endcapping-deprotection strategy as for *branch A* was applied on dibromo precursor **Br5b** in order to obtain the monomeric branch **Br8b**, which was then attached to ligand precursor **5a** by S_N2 reaction upon treatment with sodium hydride in order to give ligand **Lig4**. Here as well, the yield turned out to be astonishingly low despite TLC confirming full conversion of **5a** and displaying two spots, as it was the case for **Lig3**.

Here again, in order to overcome the unexpected efficiency issues, we foresee to proceed with this project in the same way as already discussed above.

In order to obtain dimeric branch **Br10b** — similarly as stated above for *branch A* — the free thiol **Br8b** was dimerized with the monoprotected precursor **Br6b** by treatment with NaH, and deprotected with trifluoroacetic acid in presence of triethylsilane. The obtained **Br10b** was subsequently attached to ligand core **5a** through SN₂ reaction towards ligand **Lig6**. In this case, the yield was, in comparison with the SN₂ coupling of **Br8b** and **5a**, much higher, which has remained inexplicable so far.

If needed, this procedure as well can be performed at will in order to increase the length of the ligand chains.

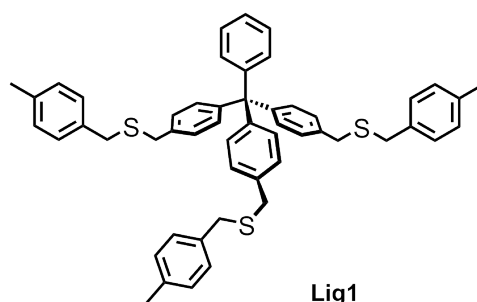
3.3 Synthesis and Characterization of the Gold Nanoparticles

The formation of Au NPs stabilized by the here presented ligands, **Lig1-5**, was carried out with a modified *Brust-Schiffrin*^{9,10} protocol, using DCM instead of toluene as a solvent and eluent for purification by manual GPC. This procedure has proven to be reliable in the synthesis of small particles stabilized not only by thiols, but also by thioethers.^{32-36,44} The initially planned target trithiol **6a** was not used for ligand stabilization for its inability to dissolve in DCM or toluene as discussed above.

For the preparation of Au NPs, hydrochloroauric acid was dissolved in deionized water, and transferred into DCM using TOAB as a phase transfer catalyst. The completion of this step could be monitored by the naked eye, as the aqueous solution of hydrochloroauric acid is yellow, while when transferred to DCM, the organic phase turns dark orange, and the aqueous phase is colorless. At room temperature this step took in the vicinity of 15 minutes. Once the hydrochloroauric acid had transferred to the organic phase, the respective ligand dissolved in DCM was added under vigorous stirring. The stoichiometry of each compound were chosen such that for each stabilizing sulfur per ligand, one equivalent of hydrochloroauric acid was added, for reasons of comparability with former studies.^{32-34,36,44,69} After stirring for 15 minutes, the gold precursor was reduced upon quick addition of an aqueous solution of sodium borohydride, after which an immediate color change of the organic phase from orange to dark brown was observed. The mixture was stirred for another 15 minutes, before the organic phase was carefully extracted, and concentrated until a minimum amount of solvent (approximately 0.5 ml) remained by bubbling with a steady argon stream. In order to remove the remaining TOAB, the crude NPs were precipitating by addition of EtOH, centrifuged for 25 minutes with 4000 rpm, at 5 °C. The brown supernatant was decanted, and the centrifugation in EtOH was repeated twice

more. The Au NPs were purified by manual GPC, using DCM as an eluent. Collection of small fractions and subsequent UV/Vis spectroscopy allowed the identification of fractions containing excess of ligand. The combined pure fractions were dried *in vacuo* at 30 °C to recover a dark brown solid. ¹H-NMR spectra of the purified particles showed strong contamination of grease and silicon grease residue which were not present in the ligand before the particle synthesis. We believe that these impurities come either from the GPC beads or from the glassware used for it. In order to remove grease impurities, the particles were thoroughly washed and sonicated.

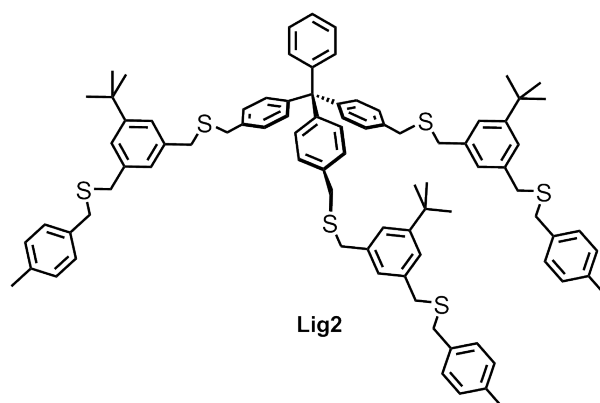
3.3.1 Au NPs from Lig1 (Au-Lig1)



Lig1 did not succeed in the synthesis of solution-stable Au NPs, although no agglomerates of particles precipitated during the synthesis. During the centrifugation procedures already, a color change from dark brown to black was observed — a first indication that the ligands do not succeed in stabilizing the Au NPs in a favorable fashion; or do not provide a high enough solvation shell in order to be redissolved. This finding was confirmed by trying to redissolve the particles in DCM, which was not possible. For this reason, these particles were not worked on further.

We assign the weak solubility of these particles to the architecture of **Lig2** that bears no bulky *tert*-butyl groups that would provide a larger solvation shell as well as more electronic repulsion between the NPs. Another explanation can be given by the low number of thioethers that do not provide strong enough stabilization of the gold cores, since the binding of thioethers to gold is significantly weaker in comparison to thiols.⁵⁵

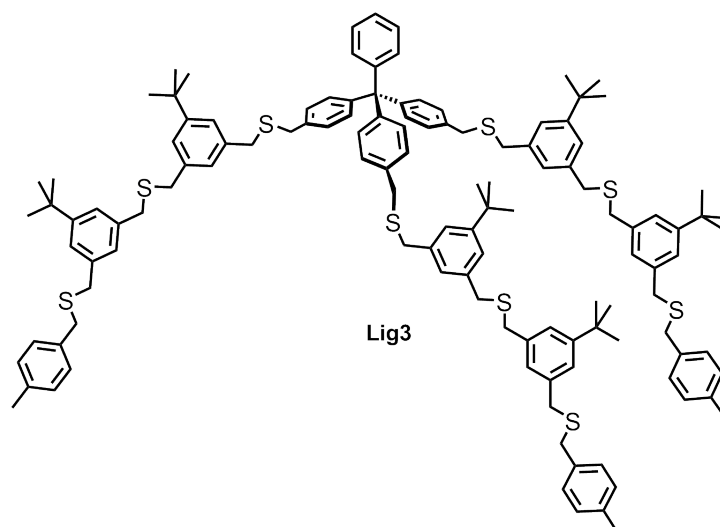
3.3.2 Au NPs from Lig2 (Au-Lig2)



Unlike **Au-Lig1**, Au NPs made from **Lig2** retained their brown color upon centrifugation, but were only weakly redissolvable in DCM after removal of the EtOH supernatant. The greater part of the particles remained undissolved, while the organic phase acquired a light brown color, showing that a few particles were in solution. Also, the few dissolved particles or small agglomerates could not be purified by manual GPC, since they were adsorbed by the beads upon application.

As is it the case for **Au-Lig1**, we believe that — despite the presence of three *tert*-butylic groups per ligand — the lack of more solvation shell- and repulsion-providing groups hinders the good solubility in DCM for this ligand. The light brown color of the organic phase, however, indicates that a better solubility was achieved by insertion of *tert*-butylic groups, albeit the delivered repulsion effect was only weak; or that the higher number of possible S-Au bonds offers enhanced stability of the gold cores.

3.3.3 Au NPs from Lig3 (Au-Lig3)



Bearing 6 *tert*-butylic groups and 9 thioethers, **Lig3** provided good enough solubility and binding to the gold core for the resulting Au NPs to be completely redissolvable in DCM after centrifugation. It is important, nevertheless, to point out that a 10 second exposure to ultrasonication was needed in order to redissolve all particles. Upon purification by manual GPC, a considerable fraction of the crude mixture, however, was adsorbed by the GPC beads, and thus could not be further analyzed.

UV/Vis absorption showed no distinct plasmon band except for a slight shoulder around 500 nm, although the measured solution was highly concentrated (see figure 8), suggesting a particle size below 2 nm.¹² From TEM micrographs, a particle size of 1.32 ± 0.37 nm was found, suggesting a rather monodisperse size distribution as can be seen in figure 9. Also, the particles showed no tendencies to clog or to form agglomerates at this point; both of which indicate that **Lig3** provides both: good solubility and stabilization of **Au-Lig3**.

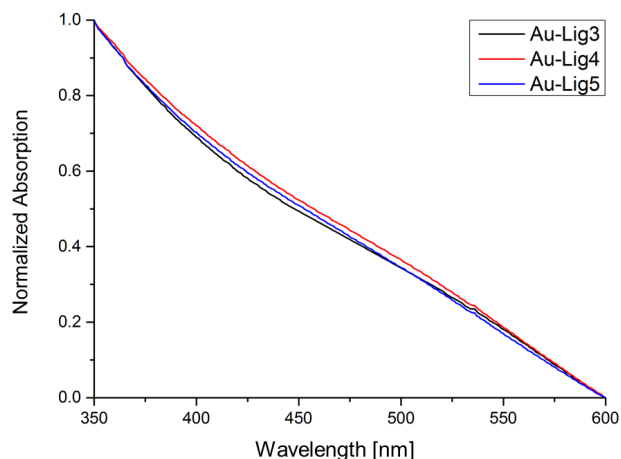


Fig. 8: Normalized UV/Vis absorption spectra of **Au-Lig3-5** in the region of interest. The similarity of all three spectra suggests a similar size for the three different synthesized particles, as was confirmed by particle diameter measurements from TEM (see figures 9, 11 and 14).

Despite the initial good solubility, after five days of storage at room temperature, under

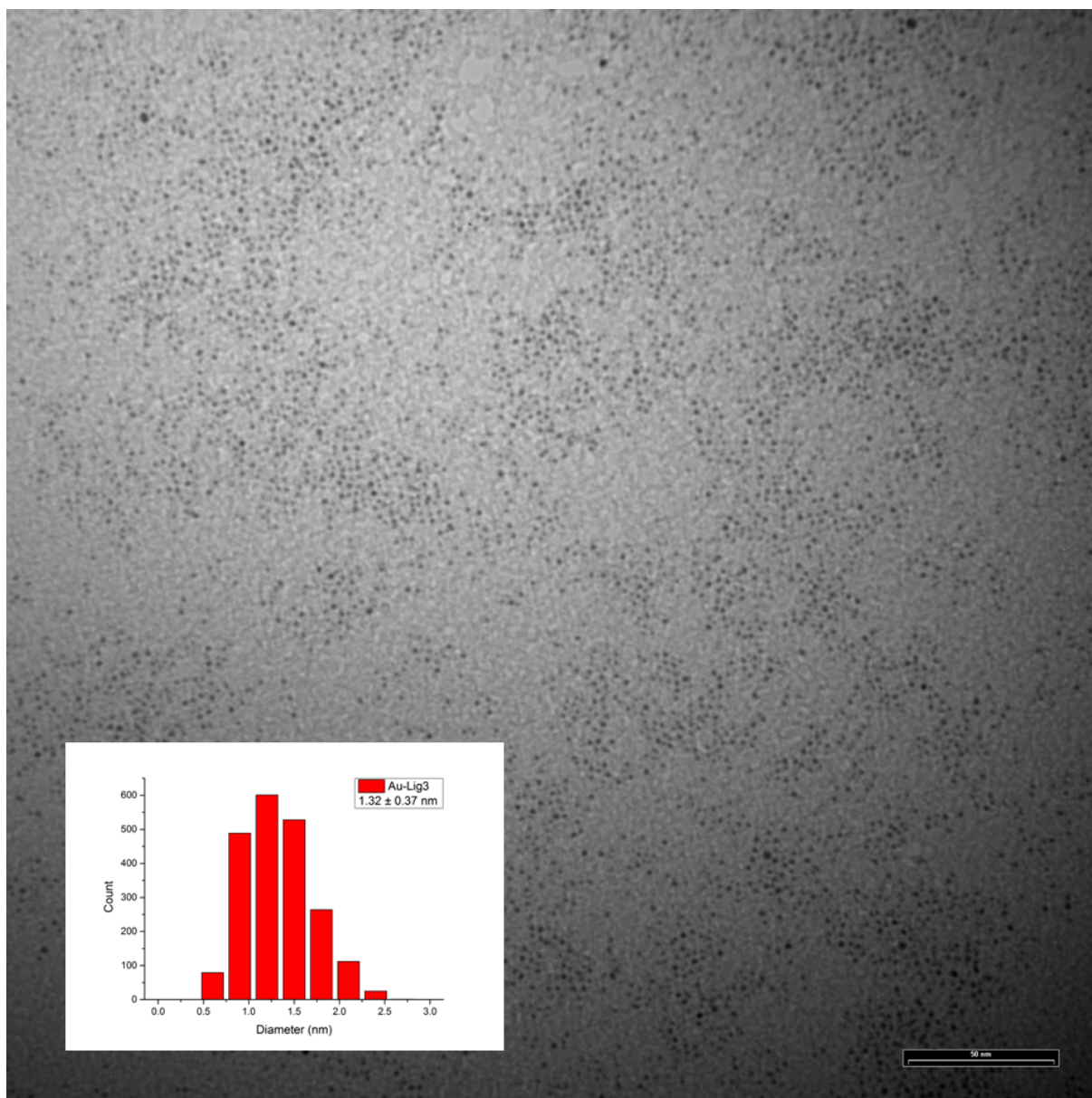


Fig. 9: Representative TEM picture of **Au-Lig3** (scale bar: 50 nm); inset: size distribution of **Au-Lig3**.

ambient conditions in dried state, the particles were not completely redissolvable in DCM any more. A fraction remained undissolved and a dispersion of black particles visible by the naked eye was observed. Even several minutes of ultrasonication did not alter the incapability of **Au-Lig3** to be dissolved again, indicating that **Lig3** does not offer reliable long-term stability of Au NPs. The observation of dimeric *branch A* offering higher stability to Au NPs leads us to the suggestion that even longer branches of this type will increase the solubility as well as the stability of the NPs.

TGA was not performed successfully as too little **Au-Lig3** was obtained from particle synthesis. Further, we suspect that the actual outcome was strongly altered through the above mentioned change in redissolvability of the particles, and is therefore useless.

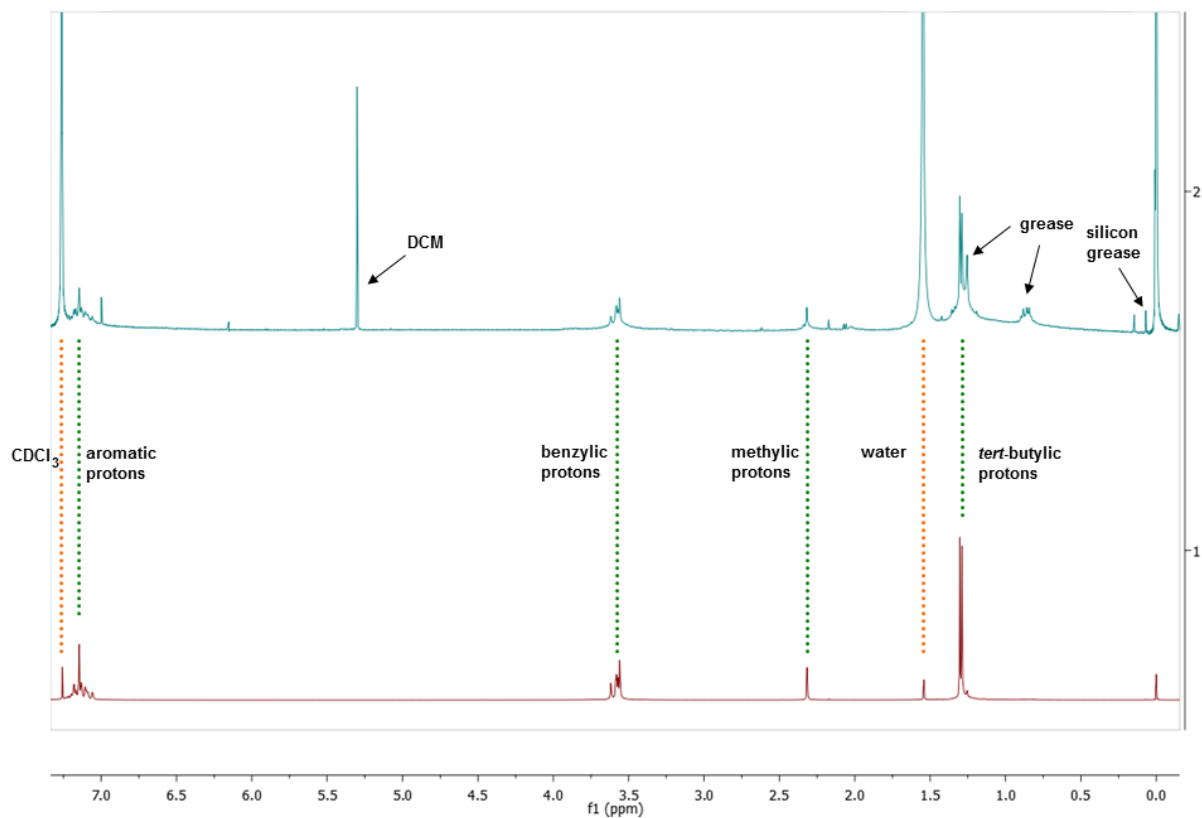
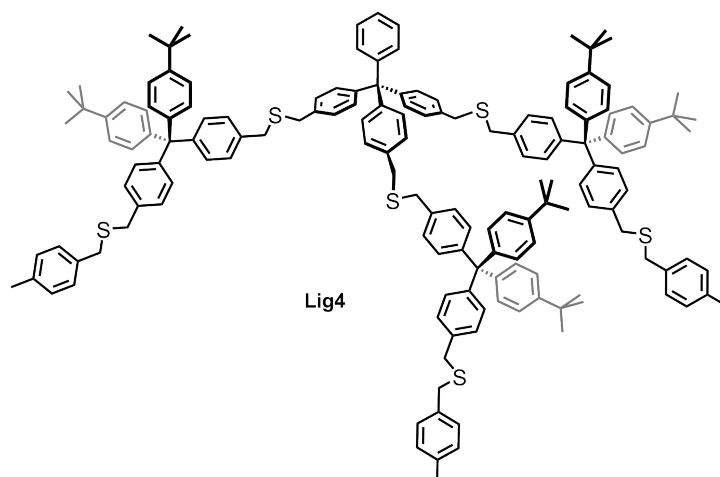


Fig. 10: Above: ¹H-NMR spectrum of **Au-Lig3**; below: ¹H-NMR spectrum of **Lig3**.

¹H-NMR spectrum of **Au-Lig3** showed the characteristic broadening³³ of the signal of **Lig3** after binding to the Au core, as can be seen in figure 10.

3.3.4 Au NPs from Lig4 (Au-Lig4)



These particles readily redissolved in DCM after centrifugation; much in contrast to **Au-Lig2** which have the same number of thioether binding units, but offer less solubility- and repulsion-enhancing *tert*-butyl groups. Further, the biting angle provided by branch **Br8b** is considerably larger compared with branch **Br3a**, and the ligand shell provided by **Lig4** is also considerably thicker. Even after several days of storage under ambient conditions in dried state, the particles' solubility was conserved, indicating that **Lig4** stabilizes the particles in a more durable and reliable fashion as **Au-Lig3**. These findings support our initial expectation that ligands with thicker ligand shell and high number of bulky, solubility- and repulsion-enhancing substituents generate more stable and more easily dissolvable particles than ligands with thin ligand shell and less *tert*-butylic substituents.⁵⁶ After two weeks of storage, however, these particles as well showed first signs of solubility issues, which suggests that longer branches are needed in order to grant long-term stability of Au NPs.

Purification by manual GPC could be losslessly achieved. Similarly to **Au-Lig3**, these particles showed no distinct absorption peak in UV/Vis spectroscopy peak despite high sample concentration as can be taken from 8, indicating a similarly small particles size, as also did the brown color. TEM and subsequent particle size measurements performed with the taken pictures were consistent with this suggestion, as a particle size of 1.14 ± 0.33 nm was found (see figure 11).

¹H-NMR spectrum of **Au-Lig4** showed the characteristic broadening of the ¹H-NMR spectrum of **Lig4** after binding to the Au core, as can be seen in figure 12.

As it was the case for **Au-Lig3**, TGA for **Au-Lig4** could not be successfully completed. Here again, we make the lack of long-term stability responsible for what we believe to be strongly altered results.

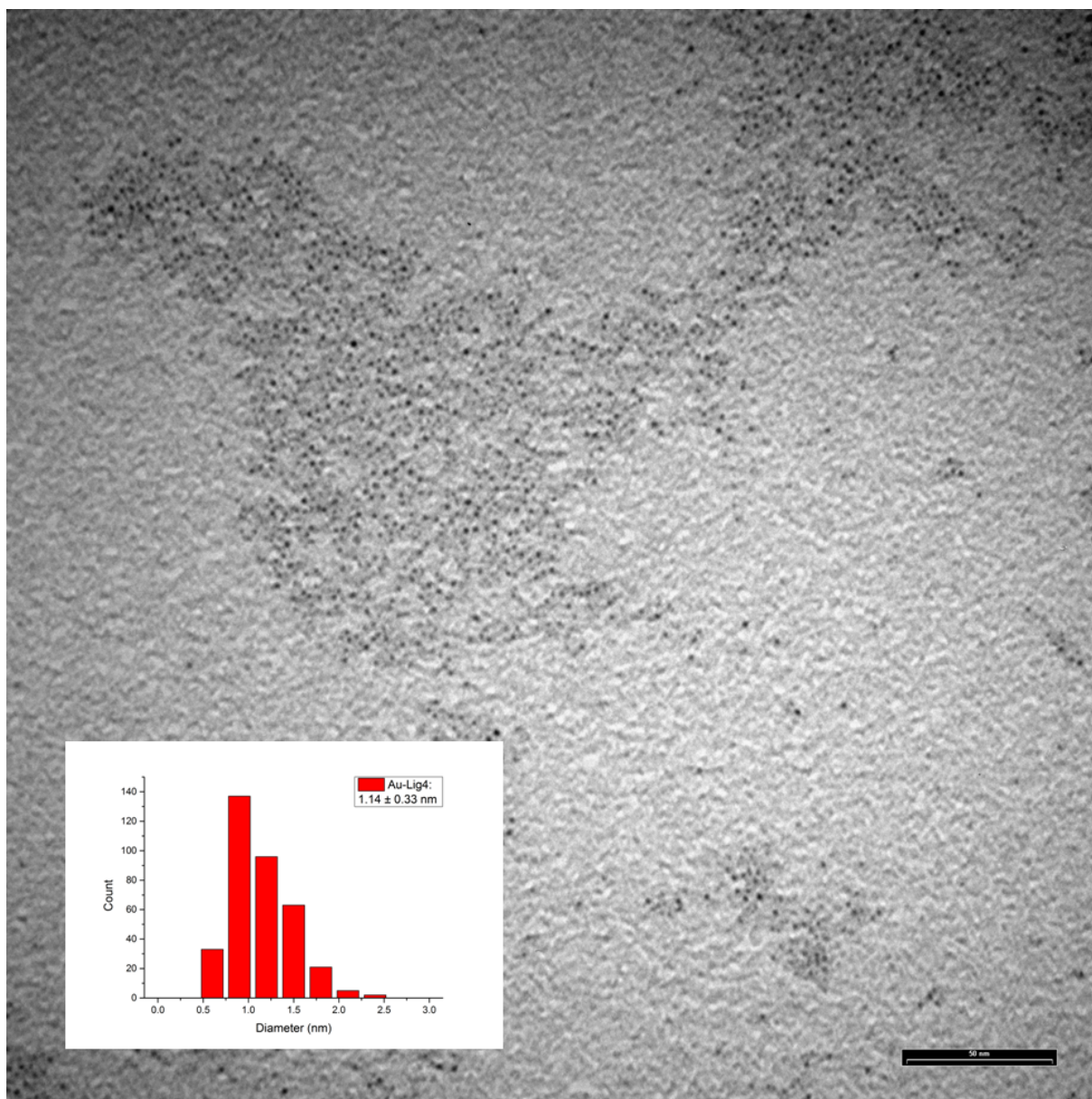


Fig. 11: Representative TEM picture of **Au-Lig4** (scale bar: 50 nm); inset: size distribution of **Au-Lig4**.

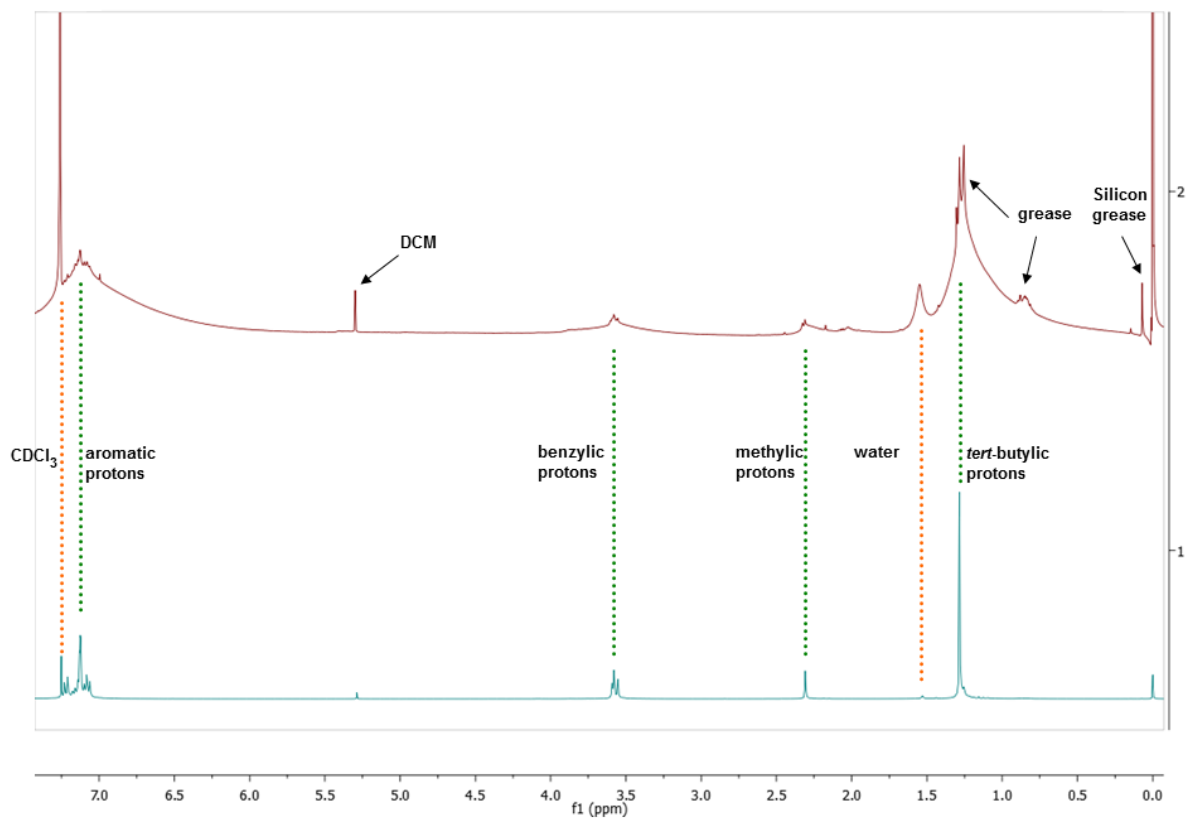
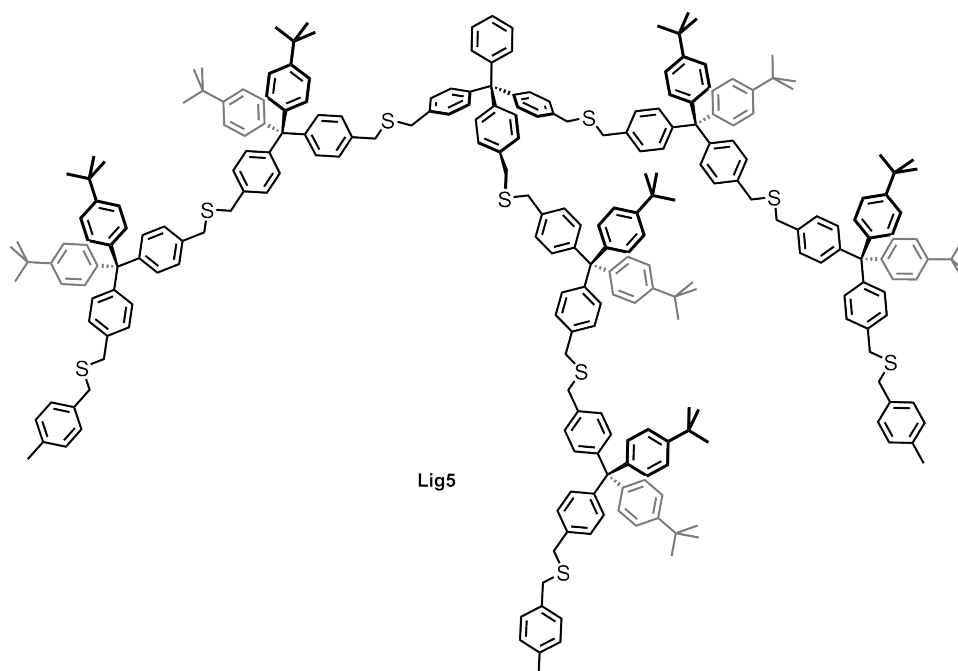


Fig. 12: Above: $^1\text{H-NMR}$ spectrum of **Au-Lig4**; below: $^1\text{H-NMR}$ spectrum of **Lig4**.

3.3.5 Au NPs from Lig5 (Au-Lig5)



As it was already the case for **Au-Lig4** and was thus expected, particles made from **Lig5** easily redissolved in DCM after centrifugation. Even after several days storage under ambient conditions in dried state, the particles' solubility was conserved, indicating that **Lig5** as well stabilizes the particles in a durable and reliable fashion. Here as well, purification by manual GPC could be losslessly achieved and UV/Vis spectroscopy showed no absorption peak (see figure 8), indicating a small particles size, as also did the brown color. TEM and particle size measurements performed with the taken pictures gave a particle size of 1.16 ± 0.29 nm (see figure 14).

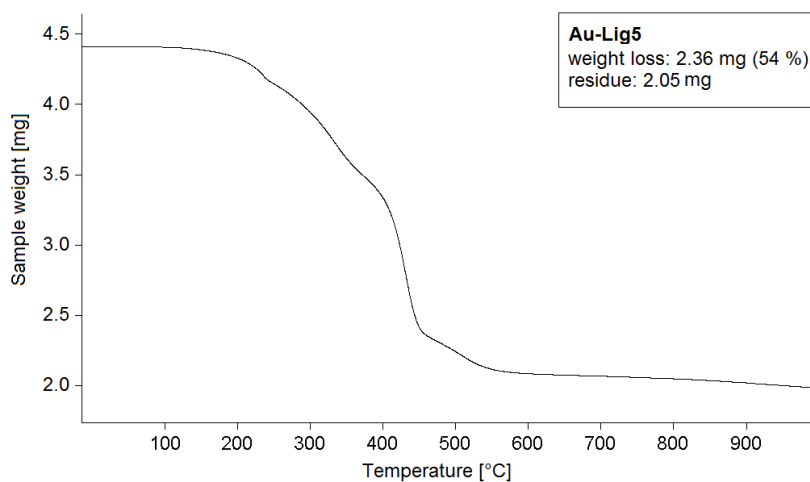


Fig. 13: Weight loss diagram of **Au-Lig5**.

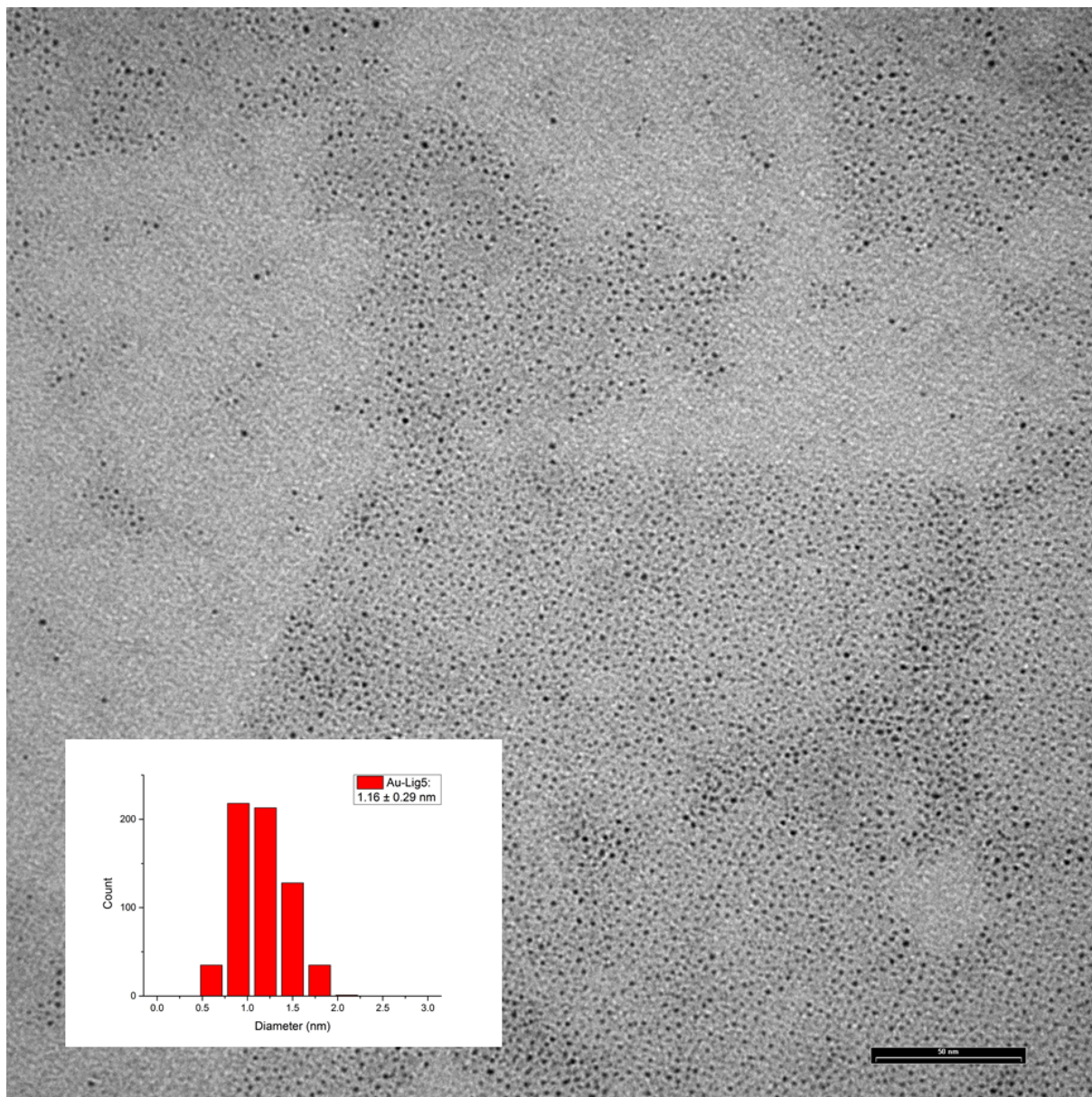


Fig. 14: Representative TEM picture of **Au-Lig5** (scale bar: 50 nm); inset: size distribution of **Au-Lig5**.

TGA gave a total weight loss of 54 % (see figure 13) which corresponds in our case to a Au-to-ligand-ratio of approximately 18, suggesting that particles with a diameter up to 0.9 nm are stabilized by only one ligand, while average-sized particles are stabilized by two ligands. From the weight loss, we calculated a particle synthesis yield of 72 % with respect to gold. To calculate these numbers, we assumed a spherical particle shape, that all organic material had been removed upon heating and didn't take grease, silicon grease or solvent impurities into account. Further, we took the bulk density of gold to calculate the number of atoms per particle. Our findings are consistent with the studies by Peterle *et al.*³² It is, nevertheless, of utmost importance — for the sake of scientific correctness — to emphasize that these data come from a single measurement and are very likely to be subject to a broad variety of error sources. Note:

all material was used for a single TGA measurement; its reproducibility is thus not given at the time.

$^1\text{H-NMR}$ spectrum of **Au-Lig5** showed the characteristic broadening of the $^1\text{H-NMR}$ spectrum of **Lig5** after binding to the Au core, as can be seen in figure 15.

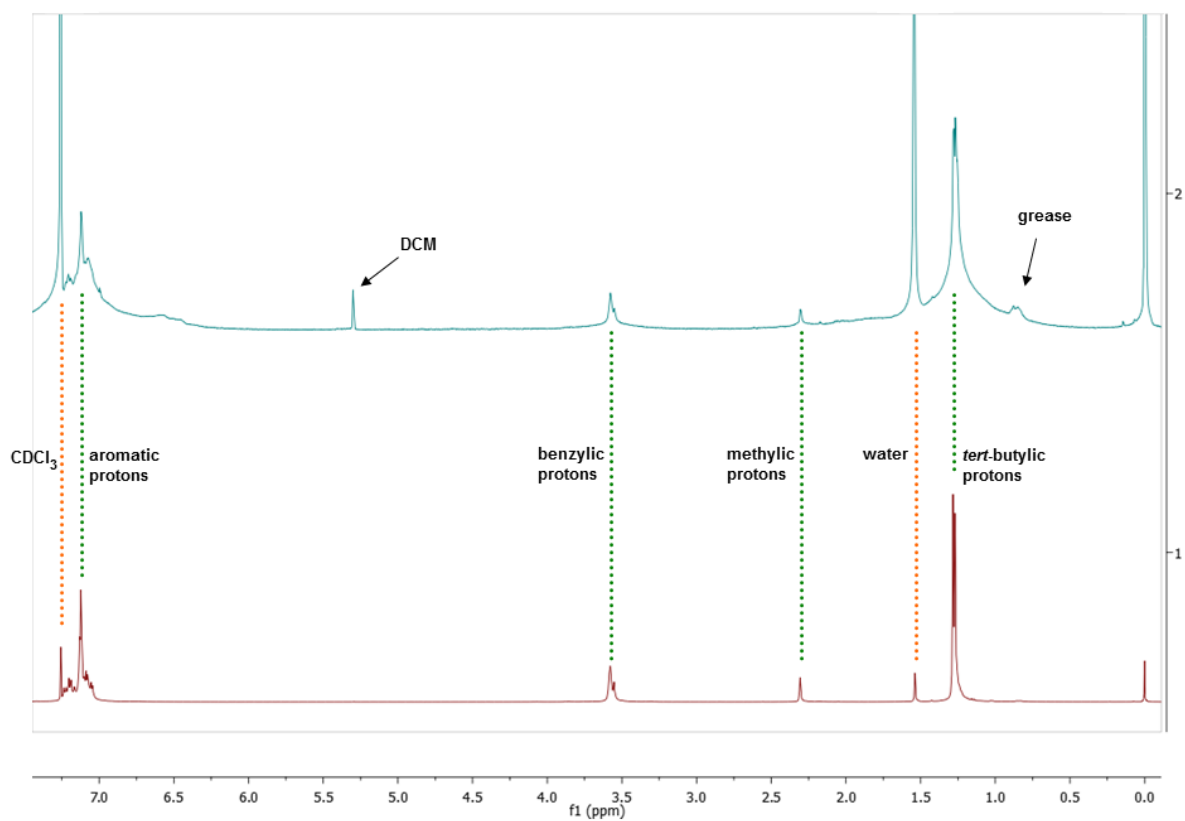


Fig. 15: Above: $^1\text{H-NMR}$ spectrum of **Au-Lig5**; below: $^1\text{H-NMR}$ spectrum of **Lig5**.

4 Conclusions and Outlook

Within this master thesis, a synthetic route towards a central unit for the synthesis of tripodal thioethers as well as three-armed oligomeric derivatives of which for the stabilization of Au NPs has been established. Three synthetic routes have been compared, revealing that *route A* is the most promising, paving the way towards functionalization, while *route B* lacks in its versatility and *route C* could not be completed due to reaching dead end halfway through its path. Two different oligomeric side chains of variable length have successfully been introduced to the central tripodal linking compound, enabling the synthesis of temporarily solution-stable Au NPs, which lost their stability within a few days in the case of **Au-Lig3** or a few weeks in the case of **Au-Lig4** respectively and long-term stable Au NPs as it is the case for **Au-Lig5**. These findings suggest that not the number of S-Au bonds, but rather the thickness of the ligand shell as well as the number of solvation shell- and electronic repulsion-providing *tert*-butyl substituents play the leading part in the synthesis of solution-stable particles. For the sake of better clarity over this assertion, however, the continuation of this work should include the insertion of longer side-chains to the central unit. The resulting Au NPs were characterized by UV/Vis spectroscopy in respect to their absorption spectrum and TEM in order to gain insight on their size distribution. For all successfully stabilized particles, similar sizes and rather narrow size-distributions were found, leading to the unanswered question if the particle size and the branch length are in any correlation. In order to gain full insight on this dependence — that is, if there is any — we strongly emphasize again the need to introduce longer side-chains. TGA investigations on **Au-Lig5** showed that typically two ligands were needed in order to stabilize one NP, using **Lig-5**. Investigations of the thermostability of the here presented Au NPs have not been performed so far and are subject to further research.

Additionally to the above mentioned and needed studies on the elongation of the branches, more efficient ways of attaching them to the central tripodal unit should be investigated on; such as introducing a branch monomer to the central unit and perform the elongation-deprotection procedure from there on. Further, as a next step towards electronic applicability of the here proposed Au NPs, introducing an electronically addressable functional group in *p*-position of the unfunctionalized phenyl moiety of the central unit should be performed in future research. In order to succeed in the completion of monofunctionalized Au NPs even, longer branches towards single-ligand stabilized particles should as well be introduced.

5 Experimental

5.1 General Information

Reagents and Solvents

All chemical were used as received without any further purification, unless stated differently. Dry Solvents were purchased from *Fluka* or *Acros*. NMR solvents were obtained from *Cambridge Isotope Laboratories, Inc.* (Andover, MA, USA).

¹H-Nuclear Magnetic Resonance

All ¹H-NMR spectra were measured at room temperature with a *Bruker DPX-NMR* (400 MHz) spectrometer. All ¹³C-NMR spectra were measured at room temperature with a *Bruker DPX-NMR* (101 MHz) spectrometer. Chemical shifts (δ) are reported in parts per million (ppm) relative to residual solvent peaks or TMS. Coupling constants, J are given in Hz. The multiplicities are written as: s = singlet, d = doublet, t = triplet, q = quartet, m = multiplet and br = broad.

Mass Spectrometry

MALDI-TOF analyses were performed on a *Bruker microflex* system, using a anthracenethiol matrix. GC/MS analyses were performed on a *Shimadzu GCMS-QP2010 SE* gas chromatography system with a *ZB-5HT inferno* column (30 mm x 0.25 mm x 0.25 mm), at 1 ml/min He-flow rate (split = 20:1) with a *Shimadzu* mass detector (EI 70 eV).

Thin Layer Chromatography

For TLC, *silica gel 60 F254* glass plates with a thickness of 0.25 mm from *Merck* were used. The detection was observed with a UV-lamp at 253 nm or 366 nm.

Column Chromatography

Column chromatography was performed with *SiliaFlash P60* from *SILICYCLE*[®] with a particle size of 40 - 63 μm (230 - 400 mesh).

Gel Permeation Chromatography

Automated GPC was performed on a *Prominence* System from *Shimadzu* with SDV preparative columns from *Polymer Standards Service* (two columns in series: 20 mm x 600 mm each; exclusion limit: 30000 g/mol) using chloroform as an eluent. Manual GPC was performed with Bio-Rad Bio-Beads S-X1 600-14000 g/mol using DCM as eluent.

UV/Vis Spectroscopy

UV/Vis spectra were recorded on a *Shimadzu* UV 1800 spectrophotometer in DCM.

Transmission Electron Microscopy

TEM was performed on a *Philips* CM100 transmission electron microscope, using a filament voltage of 80 kV. Electron micrographs were recorded on a 2000x2000 pixel charge-coupled device camera *Veleta* from *Olympus*.

Particle diameter

The NP diameters were measured using a portable copy of *imageJ*ⁱⁱⁱ. The TEM micrographs were transferred into black and white using the function *Threshold*. The particles were measured with *Analyze particles* using the following settings: area 0.4 nm²-infinity; circularity 0.9-1 in order to exclude noise and agglomerated particles.

Thermogravimetric Analysis

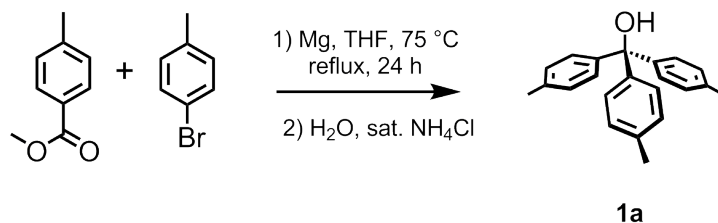
TGA was performed on a *Mettler Toledo* TGA/SDTA851 with a heating range of 25 °C to 950 °C with a heating rate of 10 °C/minute.

ⁱⁱⁱ<http://imagej.nih.gov/ij/>, as of Feb 25 2015

5.2 Synthetic Part

5.2.1 Synthetic Route A

- **Tris(*p*-tolyl)methanol (**1a**)**⁷⁰



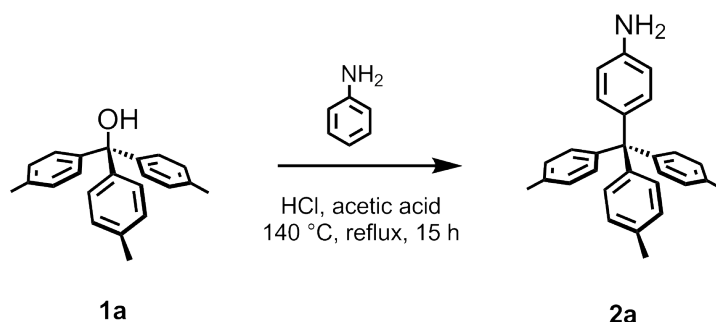
In a dry degassed 500 ml three-neck flask equipped with rubber septum, reflux condenser and addition funnel, Mg turnings (2.02 g, 83.2 mmol, 2.5 eq) were suspended in 20 ml dry degassed THF under argon atmosphere. 4-bromotoluene (14.2 g, 83.2 mmol, 2.5 eq) dissolved in 20 ml dry degassed THF were added drop-wise. In order to activate the *Grignard* reagent, one pellet of iodine was added to the mixture, which was subsequently stirred for three hours. Methyl *p*-toluate (5 g, 33.3 mmol, 1 eq) was dissolved in 20 ml dry degassed THF and added to the mixture, which was then allowed to stir at 75 °C for 24 hours. After cooling to room temperature, saturated aqueous NH₄Cl and water were added. The aqueous phase was washed twice with TBME. The combined organic phases were washed twice with water, dried over MgSO₄ and the solvent was evaporated. The crude product was subjected to column chromatography (n-hexane 5:1 DCM) to obtain a white solid (9.87 g, 32.7 mmol, 98 %).

¹H-NMR (400 MHz, Chloroform-d): δ = 7.17 – 7.12 (m, 6H), 7.09 (m, 6H), 2.70 (s, 1H), 2.32 (s, 9H).

¹³C-NMR (101 MHz, Chloroform-d): δ = 144.35, 136.74, 128.19, 81.64, 21.06.

GC/MS: 302.1 (13 %), 285.1 (12 %), 284.1 (30 %), 212.05 (12 %), 211.05 (75 %), 183.05 (23 %), 182.05 (37 %), 120 (11 %), 119.05 (100 %), 91.05 (39 %), 65.05 (10 %).

• 4-(Tris(p-tolyl)methyl)aniline (**2a**)⁵⁸



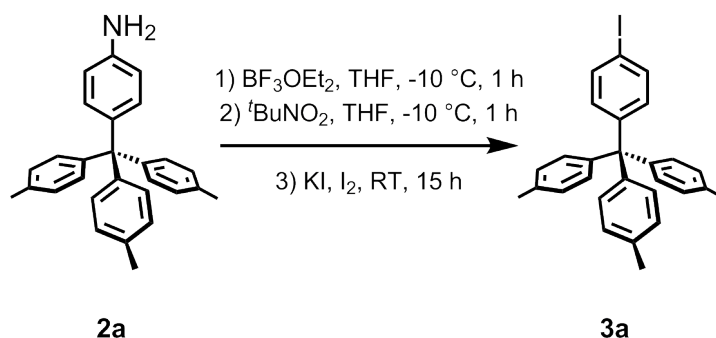
To a 250 ml two-neck flask, freshly distilled aniline (10.3 ml, 113 mmol, 4.75 eq) was added and dissolved in 5.8 ml concentrated HCl and 50 ml AcOH. Precursor **1a** (7.2 g, 23.8 mmol, 1 eq) was added portion-wise. The mixture heated to 140 °C and refluxed over night, then allowed to cool to room temperature. The volatile was evaporated by rotavapor, the remaining solid was dissolved in DCM and neutralized with 1 M NaOH. The organic phase was washed three times with water, dried over MgSO₄, and the solvent was evaporated. The crude product was subjected to column chromatography (n-hexane 1:1 EtOAc with 1 % Et₃N) and was recrystallized from hot hexane in order to afford a pale solid (5.1 g, 57 %).

¹H-NMR (400 MHz, Chloroform-d): δ = 7.08 (m, 6H), 7.02 (m, 6H), 6.98 – 6.93 (m, 2H), 6.57 – 6.52 (m, 2H), 3.55 (s, 2H), 2.30 (s, 9H).

¹³C-NMR (101 MHz, Chloroform-d): δ = 144.72, 144.01, 137.55, 135.08, 132.02, 131.02, 128.10, 114.19, 63.31, 21.00.

GC/MS: 377.1 (33 %), 287.1 (212 %), 286.1 (100 %), 194.0 (12 %).

• 4-Iodophenyl-tris(*p*-tolyl)methane (**3a**)⁵⁸



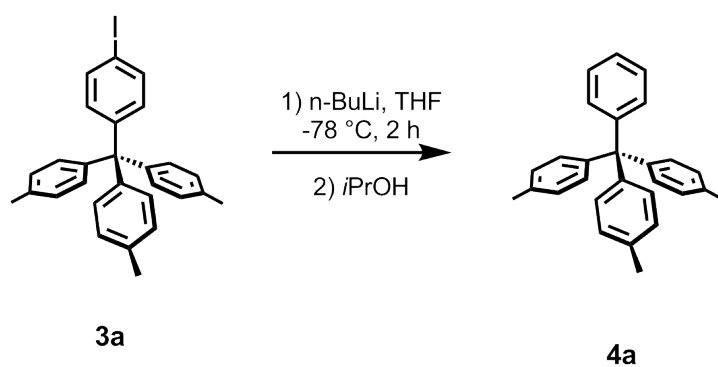
To a dry 250 ml two-neck flask, equipped with a thermometer and a rubber septum, BF_3OEt_2 (1.34 ml, 10.6 mmol, 2 eq) was added and cooled to $-10\text{ }^\circ\text{C}$. Precursor **2a** (2 g, 5.3 mmol, 1 eq) dissolved in 50 ml DCM was added drop-wise, and the mixture was stirred for 1 h at $-10\text{ }^\circ\text{C}$. The same procedure was repeated with $^t\text{BuNO}_2$ (1.11 ml, 9.28 mmol, 1.75 eq). After addition of KI (1.32 g, 7.95 mmol, 1.5 eq) and I_2 (1.75g, 6.89 mmol, 1.3 eq), the mixture was allowed to warm up to room temperature gradually, and was then stirred for 12 hours at constant temperature. The reaction mixture was quenched with saturated aqueous solution of $\text{Na}_2\text{S}_2\text{O}_3$. The aqueous phase was washed twice with DCM, the combined organic phase was washed twice with water, and dried over MgSO_4 . The crude product was isolated after column chromatography (cH 50:1 EtOAc) as a white solid (1.31 g, 2.7 mmol, 51 %).

$^1\text{H-NMR}$ (400 MHz, Chloroform-*d*): $\delta = 7.55 - 7.49$ (m, 2H), $7.09 - 7.00$ (m, 12H), $6.99 - 6.94$ (m, 2H), 2.29 (s, 9H).

$^{13}\text{C-NMR}$ (101 MHz, Chloroform-*d*): $\delta = 147.34, 143.70, 136.52, 135.51, 133.19, 130.86, 128.34, 91.62, 63.79, 20.99$.

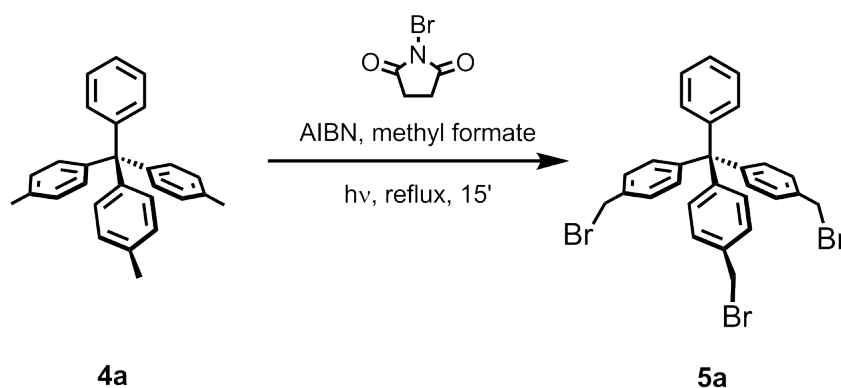
GC/MS: 488.9 (14 %), 487.9 (40 %), 472.9 (11 %), 397.9 (25 %), 396.9 (100 %), 361.1 (11 %), 286.1 (17 %), 285.1 (70 %), 270.0 (15 %), 269.0 (14 %), 255.0 (25 %), 253.0 (11 %), 239.0 (16 %), 193.0 (18 %), 179.0 (15 %), 178.0 (21 %).

From Precursor 3a



To a dry degassed 10 ml Schlenk tube, precursor **3a** (720 mg, 2.05 mmol, 1 eq) was added and dissolved in 20 ml dry THF under argon atmosphere. The mixture was cooled to -78 °C. 60 % n-BuLi in n-hexane (1.92 ml, 3.07 mmol, 1.5 eq) was added. The mixture was stirred at -78 °C for 2 hours, then quenched upon addition of 25 ml of *i*PrOH. The crude mixture was washed three times with water, dried over MgSO₄, and the volatile evaporated *in vacuo*. The crude product was subjected to column chromatography (*c*-hexane 50:1 EtOAc) to afford a pale yellowish solid (500 mg, 93 %).

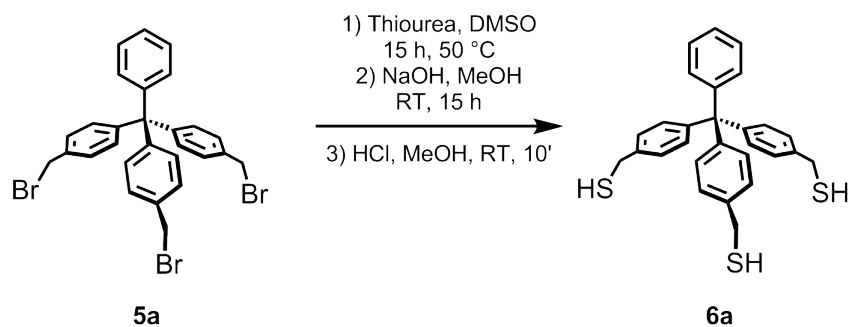
• Tris(p-bromomethylphenyl)methylbenzene (**5a**)⁶¹



A dry, degassed 500 ml two-neck flask was equipped with a reflux condenser and a glass stopper. Precursor **4a** (1.87 g, 5.16 mmol, 1 eq), N-Bromosuccinimide (5.51 g, 31 mmol, 6 eq) and 2,2'-azobis(2-methylpropionitrile) (AIBN, 169 mg, 1.03 mmol, 0.2 eq) were suspended in 200 ml methyl formate under argon atmosphere. The suspension was bubbled with argon for 30 minutes, then illuminated with a 500 W halogen lamp. The mixture was refluxed for 30 minutes and then allowed to cool to room temperature. The precipitation was concentrated, and redissolved in DCM. The solution was washed four times with water, dried over MgSO₄, and the solvent was evaporated *in vacuo*. The crude product was subjected to column chromatography (c-hexane 3:1 DCM, gradually changing to DCM), then recrystallized from hot n-hexane 1:1 chloroform to give a white solid (1.56 g, 50 %).

¹H-NMR (400 MHz, Chloroform-d): δ = 7.30 – 7.27 (m, 6H), 7.26 – 7.20 (m, 3H), 7.20 – 7.16 (m, 8H), 4.47 (s, 6H).

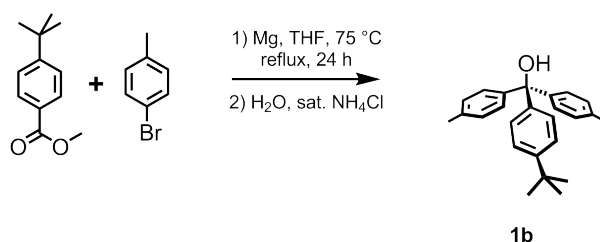
• **Tris(p-mercaptophenyl)methylbenzene (6a)**



To a dry, degassed 250 ml Schlenk tube, precursor **5a** (500 mg, 0.834 mmol, 1 eq) was added and suspended in 40 ml dry degassed DMSO. The mixture was heated to 50 °C under vigorous stirring and thiourea (952 mg, 12.5 mmol, 15 eq) was added to the mixture. After stirring for 15 hours, 50 ml degassed aqueous 1 M NaOH was added and stirred for additional 24 hours at room temperature. Upon subsequent addition of 75 ml degassed aqueous 1 M HCL, the crude product precipitated immediately. The precipitate was filtered off and washed with 1.5 l of water to remove DMSO residues. It was then rinsed with 250 ml DCM and 250 diethyl ether to remove organic impurities, yielding an insoluble pale brownish solid (332 mg, 87 %).

5.2.2 Synthetic Route B

• Bis(*p*-tolyl)-(4-(*tert*-butyl)phenyl)methanol (**1b**)⁷¹



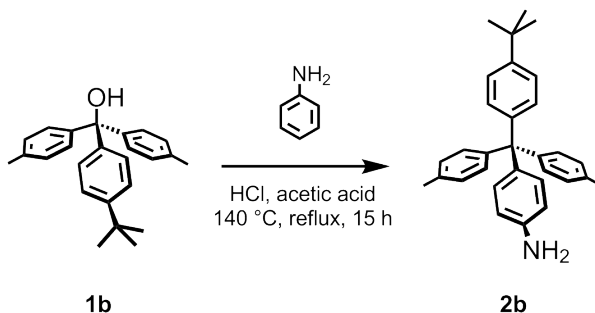
In a dry degassed 500 ml two-neck flask equipped with rubber septum, reflux condenser and addition funnel, Mg turnings (1.58 g, 65 mmol, 2.5 eq) were suspended in 20 ml dry degassed THF under argon atmosphere. 4-bromotoluene (11.1 g, 65 mmol, 2.5 eq) dissolved in 20 ml dry degassed THF were added drop-wise. In order to activate the *Grignard* reagent, one pellet of iodine was added to the mixture, which was subsequently stirred for three hours. Methyl *p*-toluate (4.72 ml, 26 mmol, 1 eq) was dissolved in 20 ml dry degassed THF and was added to the mixture, which was then allowed to stir at 75 °C for 24 hours. After cooling to room temperature, saturated aqueous NH₄Cl and water were added. The aqueous phase was washed twice with TBME. The combined organic phases were washed twice with water, dried over MgSO₄ and the solvent was evaporated. The crude product was subjected to column chromatography (n-hexane 5:1 DCM) to obtain a white solid (7.29 g, 21.1 mmol, 81 %).

¹H-NMR (400 MHz, Chloroform-d): δ = 7.30 (m, 2H), 7.19 – 7.14 (m, 6H), 7.12 – 7.07 (m, 4H), 2.70 (s, 1H), 2.33 (s, 6H), 1.30 (s, 9H).

¹³C-NMR (101 MHz, Chloroform-d): δ = 149.92, 144.42, 144.24, 136.69, 128.58, 127.88, 127.63, 124.81, 81.64, 34.50, 31.43, 21.11.

GC/MS 344.1 (12 %), 327.1 (29 %), 326.1 (70 %), 312.1 (14 %), 311.1 (34 %), 254.1 (15 %), 253.1 (72 %), 224.1 (21 %), 211.0 (30 %), 182.1 (15 %), 161.1 (27 %), 134.1 (14 %), 119.1 (100 %), 91.0 (32 %), 57.1 (34 %).

• (Bis(*p*-tolyl)-(4-(*tert*-butyl)phenyl)methyl)-*p*-aniline (**2b**)



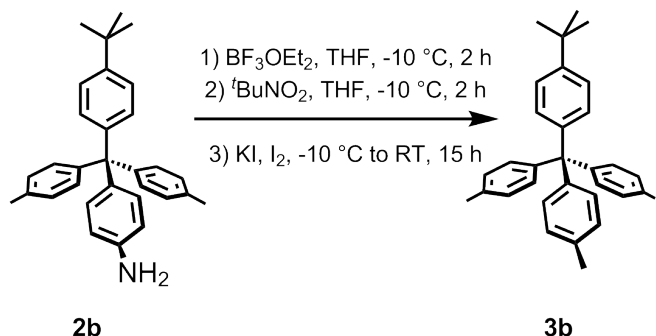
To a 250 ml two-neck flask, distilled aniline (5.57 g, 59.9 mmol, 4.75 eq) was added and dissolved in 4 ml concentrated HCl and 50 ml AcOH. Precursor **1b** (4.33 g, 12.6 mmol, 1 eq) was added portion-wise. The mixture was heated to 140 °C and refluxed for 15 hours under rigorous stirring, then allowed to cool to room temperature. The volatile was evaporated by rotavapor. The remaining solid was dissolved in DCM and neutralized with 1M NaOH. The organic phase was washed three times with water, dried over MgSO₄, and the solvent was evaporated. The crude product was subjected twice to column chromatography (n-hexane 1:1 EtOAc with 1 % Et₃N and n-hexane 1:1 DCM with 1% Et₃N) in order to afford a white solid (2.59 g, 6.2 mmol, 49 %).

¹H-NMR (400 MHz, Chloroform-d): δ = 7.21 (m, 2H), 7.11 – 7.06 (m, 6H), 7.02 (m, 4H), 6.98 – 6.94 (m, 2H), 6.58 – 6.53 (m, 2H), 3.57 (s, 2H), 2.30 (s, 6H), 1.29 (s, 9H).

¹³C-NMR (101 MHz, Chloroform-d): δ = 148.20, 144.69, 144.39, 143.93, 137.59, 135.00, 132.02, 131.02, 130.66, 127.99, 124.14, 114.11, 63.19, 34.32, 31.43, 20.96.

GC/MS 420.2 (14 %), 419.2 (40 %), 329.1 (27 %), 328.1 (100 %), 287.1 (12 %), 286.1 (45 %).

• (Di-(p-tolyl)-(4-(tert-butyl)phenyl)methyl)-p-iodobenzene (**3b**)



To a dry, degassed 250 ml two-neck flask, $\text{BF}_3\cdot\text{OEt}_2$ (573 μl , 9.54 mmol, 2 eq) was added and cooled to $-10\text{ }^\circ\text{C}$. Precursor **2b** (950 mg, 4.77 mmol, 1 eq) dissolved in 50 ml DCM was added drop-wise through a transfer needle. The mixture was stirred for 2 h at $-10\text{ }^\circ\text{C}$ at which time the same procedure was repeated with $^t\text{BuNO}_2$ (474 μl , 8.35 mmol, 1.75 eq). After addition of KI (563 mg, 7.15 mmol, 1.5 eq) and I_2 (4.93 mg, 6.20 mmol, 1.3 eq), the mixture was allowed to gradually heat up to room temperature and was then stirred for 20 hours. The reaction mixture was quenched with a saturated aqueous solution of $\text{Na}_2\text{S}_2\text{O}_3$. The aqueous phase was extracted twice with TBME. The combined organic phase was washed twice with water, dried over MgSO_4 and the volatile evaporated by rotavapor. The crude product was subjected to column chromatography (cH 50:1 EtOAc) to afford as a white solid (663 mg, 1.25 mmol, 55 %).

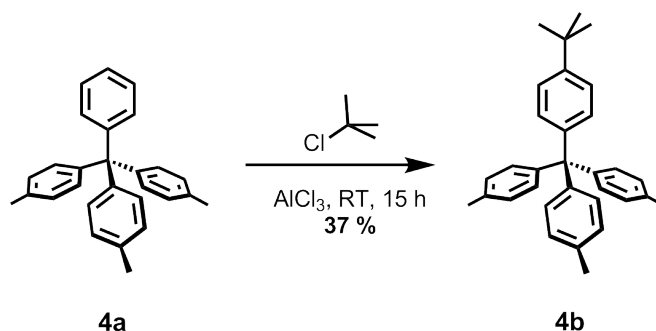
$^1\text{H-NMR}$ (400 MHz, Chloroform- d): $\delta = 7.56 - 7.51$ (m, 2H), $7.25 - 7.20$ (m, 2H), $7.09 - 7.02$ (m, 10H), $6.99 - 6.94$ (m, 2H), 2.31 (s, 6H), 1.29 (s, 9H).

$^{13}\text{C-NMR}$ (101 MHz, Chloroform- d): $\delta = 148.64$, 147.36 , 143.71 , 143.41 , 136.45 , 135.45 , 133.24 , 130.90 , 130.57 , 128.26 , 124.42 , 91.57 , 63.70 , 34.37 , 31.42 , 20.98 .

GC/MS 530.95 (17.4 %), 529.95 (43.3 %), 440 (25.2 %), 438.95 (100 %), 396.9 (42.33 %), 328.1 (30.05 %), 327.1 (89.5 %), 281 (29.95 %), 255 (19.58 %), 252.9 (18.03 %), 207.9 (17.73 %), 206.95 (69.92 %), 191 (15.79 %), 179 (16.49 %), 178 (15.7 %), 78 (25.11 %), 57.1 (29.26 %).

• **Tris(p-tolyl)-(4-(tert-butyl)phenyl)methane (4b)**

From Precursor 4a



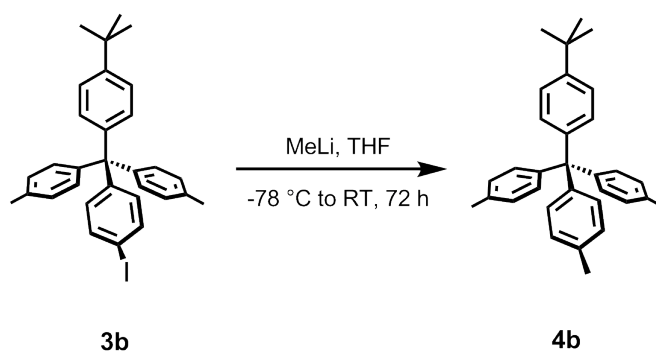
In a dry, degassed 50 ml Schlenk tube, precursor **4a** (240 mg, 0.66 mmol, 1 eq) was dissolved in 2-chloro-2-methylpropane (14.6 ml, 132 mmol, 200 eq). AlCl₃ (88.3 mg, 0.66 mmol, cat.) was added to the solution, and mixture was stirred at room temperature for 15 hours. The reaction mixture was quenched with water, and extracted twice with TBME. The combined organic phases were washed twice with water, dried over MgSO₄, and the solvent was evaporated *in vacuo*. The crude product was subjected to column chromatography (c-hexane 50:1 EtOAc) and to gel permeation chromatography (chloroform) to afford a white solid (101 mg, 37 %).

¹H-NMR (400 MHz, Chloroform-d): $\delta = 7.24 - 7.20$ (m, 2H), 7.12 - 7.07 (m, 8H), 7.05 - 7.01 (m, 6H), 2.30 (s, 9H), 1.29 (s, 9H).

¹³C-NMR (101 MHz, Chloroform-d): $\delta = 148.27, 144.40, 144.08, 135.09, 131.00, 130.63, 128.03, 124.18, 63.55, 34.31, 31.39, 20.94$.

GC/MS 418.1 (22 %), 328.1 (26 %), 327.1 (100 %), 285.1 (36 %), 269.1 (11 %), 193.0 (11 %), 179.1 (11 %).

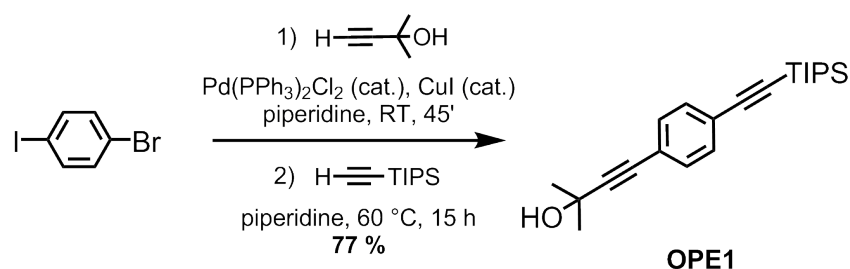
From Precursor **3b**



To a dry, degassed 25 ml Schlenk tube, precursor **3b** (672 mg, 1.27 mmol, 1 eq) was added, dissolved in 5 ml dry, degassed THF and cooled to -78 °C. After addition of MeLi (1.6 M in diethyl ether, 1.1 ml, 45.75 mmol, 36 eq), the mixture was allowed to slowly heat up to room temperature and was then stirred for 72 hours. The reaction mixture was quenched with water, and extracted three times with TBME. The combined organic phases were washed twice with water, dried over MgSO₄, and the solvent was evaporated by rotavapor to yield a pale yellowish solid (430 mg, 81 %).

5.2.3 Synthetic Route C

- 1-(TIPS-ethynyl)-4-(HOP-ethynyl)benzene (OPE1)⁶⁸

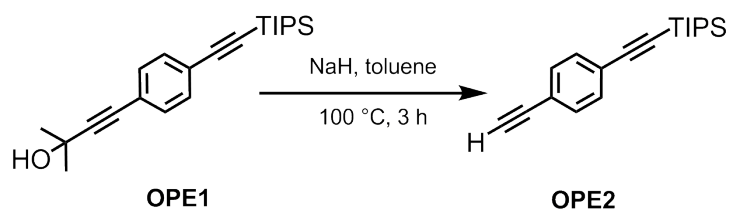


To a dry, degassed 50 ml Schlenk tube, bis(triphenylphosphine)palladium(II) chloride (372 mg, 0.53 mmol, cat.) and copper iodide (101 mg, 0.53 mmol, cat.) were added and dissolved in piperidine. The mixture was bubbled with argon for 15 minutes. 1-bromo-4-iodobenzene (1.5 g, 5.3 mmol, 1 eq) was added to the mixture which was bubbled with argon for additional 15 minutes. HOP-acetylene (544 μl , 5.57 mmol, 1.05 eq) was added to the solution. After stirring the mixture at room temperature for 45 minutes, TIPS-acetylene (1.25 ml, 5.57 mmol, 1.05 eq) was added. The mixture was heated to 60 °C and stirred for 45 minutes. The mixture was allowed to cool down to room temperature and was then diluted with EtOAc. The solvent was evaporated, and remaining black crude product subjected to column chromatography (c-hexane 10:1 EtOAc) to afford a brown oil (1.4 g, 4.1 mmol, 77 %).

¹H-NMR (400 MHz, Chloroform-d): δ = 7.41 – 7.31 (m, 4H), 3.03 (s, 1H), 1.61 (s, 6H), 1.13 (s, 21H).

¹³C-NMR (101 MHz, Chloroform-d): δ = 131.84, 131.42, 123.30, 122.76, 106.64, 95.77, 92.47, 81.78, 65.56, 31.43, 18.68, 11.32.

• 1-(TIPS-ethynyl)-4-ethynylbenzene (**OPE2**)⁶⁸

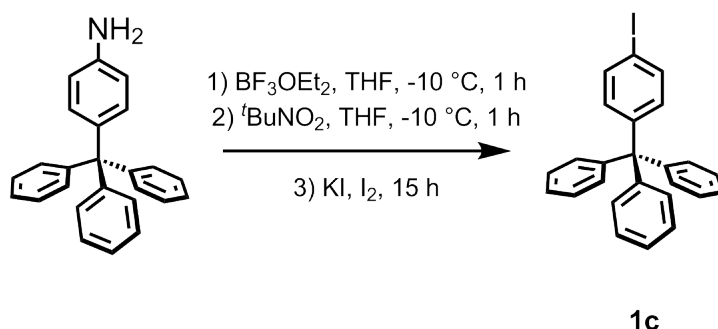


A 100 ml two-neck flask and a stirring bar were washed beforehand with sulfuric acid and rinsed with acetone. OPE-rod precursor **OPE1** (1.4 g, 4.11 mmol, 1 eq) was dissolved in 15 ml toluene, which was then bubbled with argon for 30 minutes, and then sodium hydride (60 % dispersion in oil, 904 mg, 22.6 mmol, 5.5 eq) was added to the mixture. The mixture was heated up to 100 °C and stirred for 3 hours. The mixture was filtered to remove precipitated NaOH. The solvent was evaporated and the crude product was subjected to column chromatography (n-hexane) to afford a colorless liquid (325 mg, 1.15 mmol, 33 %).

¹**H-NMR** (400 MHz, Chloroform-d): δ = 7.42 (s, 4H), 3.16 (s, 1H), 1.13 (s, 21H).

¹³**C-NMR** (101 MHz, Chloroform-d): δ = 131.90, 123.99, 121.89, 106.37, 93.00, 83.27, 78.84, 18.66, 11.29.

• 4-trityliodobenzene (**1c**)⁶³



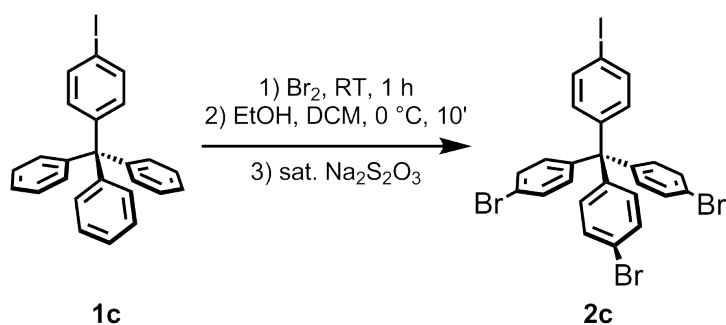
To a dry 250 ml two-neck flask, BF_3OEt_2 (1.51 ml, 11.9 mmol, 2 eq) was added and cooled to $-10\text{ }^\circ\text{C}$. 4-tritylaniline (2 g, 5.96 mmol, 1 eq) dissolved in 50 ml dry degassed DCM was added drop-wise, and the mixture was stirred for 1 hour at $-10\text{ }^\circ\text{C}$. The same procedure was repeated with $t\text{BuNO}_2$ (1.25 ml, 10.4 mmol, 1.75 eq). After addition of KI (1.48 g, 8.94 mmol, 1.5 eq) and I_2 (1.97 g, 7.75 mmol, 1.3 eq), the mixture was allowed to gradually warm up to room temperature and was then stirred for 12 hours. The reaction mixture was quenched with a saturated aqueous solution of $\text{Na}_2\text{S}_2\text{O}_3$ and extracted twice with DCM. The combined organic phase were washed twice with water and dried over MgSO_4 . Upon evaporation of the solvent, a pale solid precipitated. Recrystallization from hot acetone afforded a pale solid (1.52 g, 3.40 mmol, 57 %).

$^1\text{H-NMR}$ (400 MHz, Chloroform-d): $\delta = 7.60 - 7.55$ (m, 2H), $7.25 - 7.20$ (m, 6H), $7.20 - 7.17$ (m, 6H), $7.17 - 7.15$ (m, 3H), $7.00 - 6.96$ (m, 2H).

$^{13}\text{C-NMR}$ (101 MHz, Chloroform-d): $\delta = 148.01, 147.45, 137.61, 134.28, 132.02, 128.53, 127.06, 92.52, 65.87$.

GC/MS 446.9 (10 %), 445.9 (40 %), 369.9 (18 %), 368.9 (100 %), 243.0 (32 %), 242.0 (24 %), 241.0 (33 %), 239.0 (18 %), 165.0 (47 %).

• Tris(4-bromobenzyl)-(4-iodophenyl)methane (**2c**)⁶³

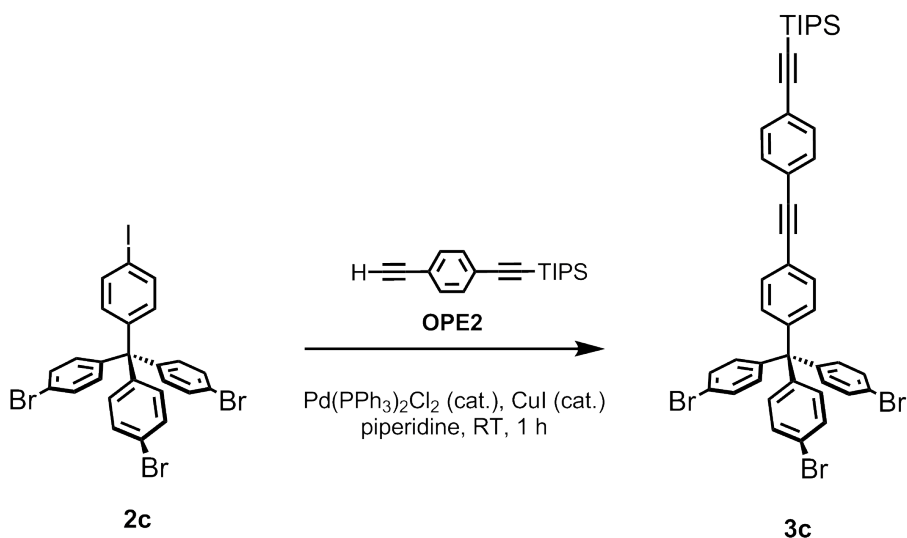


In a dry degassed 250 ml Schlenk tube, precursor **1c** (1.75 g, 3.92 mmol, 1 eq) was dissolved in bromine (7 ml, 136 mmol, 35 eq), stirred for 2 hours at room temperature, then cooled to 0 °C. 35 ml ice cold ethanol and 50 ml DCM were added to the reaction mixture. The reaction mixture was quenched by slow addition of 150 ml Na₂S₂O₂. The aqueous phase was extracted once with DCM and the combined organic fractions were washed twice with water, and dried over MgSO₄. After evaporation of the solvent *in vacuo*, the crude product was subjected to column chromatography eluting with n-hexane that was gradually changed to DCM, resulting in a white solid (2.68 g, 3.92 mmol, quant.).

¹H-NMR (400 MHz, Chloroform-d): δ = 7.63 – 7.55 (m, 2H), 7.43 – 7.36 (m, 6H), 7.04 – 6.98 (m, 6H), 6.92 – 6.84 (m, 2H).

¹³C-NMR (101 MHz, Chloroform-d): δ = 145.32, 144.53, 137.21, 132.77, 132.50, 131.23, 120.94, 63.87.

• (Tris(4-bromobenzyl)methyl)-4-(4-(TIPS-ethynyl)phenylethynyl)benzene (**3c**)



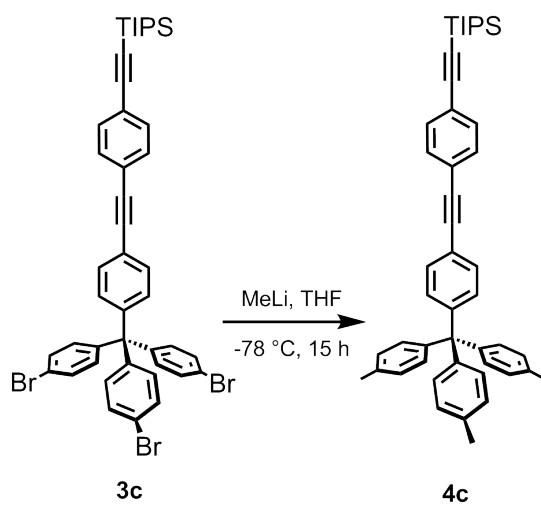
To a dry, degassed 50 ml Schlenk tube, bis(triphenylphosphine)palladium(II) chloride (18.8 mg, 0.016 mmol, cat.) and copper iodide (12 mg, 0.063 mmol, cat.) were added and dissolved in 15 ml piperidine. After bubbling with argon for 15 minutes, precursor **2c** (100 mg, 0.146 mmol, 1 eq) was added. The mixture was bubbled with argon for additional 45 minutes. OPE-rod **OPE2** (60 mg, 0.212 mmol, 1.45 eq) was added to the mixture, stirred for 3 hours at room temperature and was then diluted with EtOAc. After evaporation of the volatile, the crude product was purified by column chromatography (c-hexane 20:1 EtOAc) and subsequent automated GPC (chloroform) to afford a yellow oil (37.5 mg, 0.045 mmol, 31 %).

¹H-NMR (400 MHz, Chloroform-d): $\delta = 7.45 - 7.37$ (m, 12H), 7.13 (m, 2H), 7.06 – 7.00 (m, 6H), 1.13 (s, 21H).

¹³C-NMR (101 MHz, Chloroform-d): $\delta = 145.69, 144.53, 132.44, 131.98, 131.38, 131.17, 131.07, 130.69, 123.48, 122.90, 121.37, 120.77, 106.59, 92.93, 90.57, 89.73, 63.96, 18.68, 11.32$.

MALDI-TOF 834.8 (88 %), 835.9 (84 %), 836.8 (100 %), 837.9 (91 %), 838.9 (93 %), 839.9 (83 %), 840.9 (79 %).

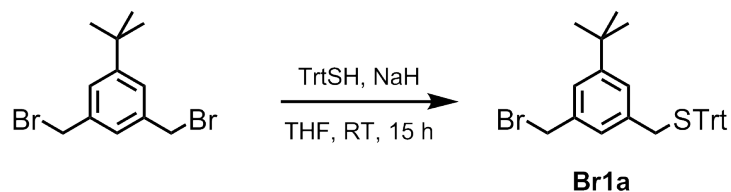
• (Tris(p-tolyl)methyl)-4-(4-(TIPS-ethynyl)phenylethynyl)benzene (**4c**)



In a dry degassed 10 ml one-neck flask, precursor **3c** (37.5 mg, 0.045 mmol, 1 eq) was dissolved in 1 ml THF. The solution was transferred to a dry, degassed 5 ml Schlenk tube. Additional 0.5 ml dry degassed THF were used to rinse the one-neck flask. The mixture was cooled to -60 °C. 1.6 M Methyllithium in Et₂O (0.2 ml, 7.39 mmol, 165 eq) was added to the reaction mixture. The mixture was allowed to stir for 12 hours and monitored by TLC throughout the process. Since no reaction was observed, it was quenched with water and given up.

5.2.4 Branch A

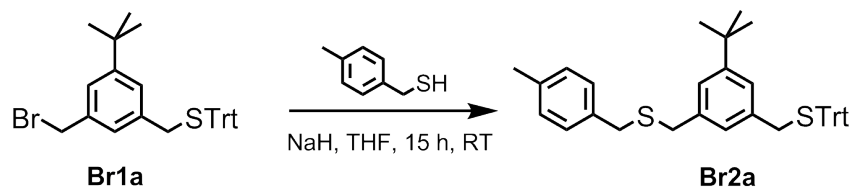
- 1-(Bromomethyl)-3-(tritylthiomethyl)-5-(tert-butyl)benzene (**Br1a**)⁶⁹



In a dry, degassed 250 ml 3-neck flask, 1-3-di-(bromomethyl)-5-*tert*-butylbenzene (1.42 g, 4.44 mmol, 1 eq) and tritylthiol (1.23 g, 4.44 mmol, 1 eq) were dissolved in 25 ml dry, degassed THF. NaH (60 % dispersed in mineral oil, 213 mg, 5.32 mmol, 1.2 eq) was added to the solution which was then allowed to stir at room temperature for 17 hours. The reaction mixture was quenched with water, then extracted three times with TBME, washed once with brine, dried over MgSO₄ and the solvent removed *in vacuo*. The crude product was subjected to column chromatography (c-hexane 10:1 DCM), yielding a white solid (820 mg, 36 %).

¹H-NMR (400 MHz, Chloroform-d): δ = 7.50 – 7.42 (m, 6H), 7.35 – 7.20 (m, 10H), 7.02 (s, 1H), 6.95 (s, 1H), 4.43 (s, 2H), 3.32 (s, 2H), 1.27 (s, 9H).

• 1-(*p*-tolylmethylthiomethyl)-3-(tritylthiomethyl)-5-(*tert*-butyl)benzene (**Br2a**)³³

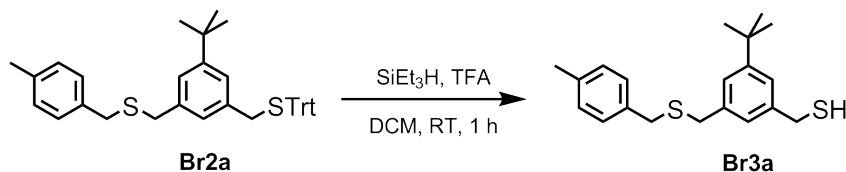


In a dry, degassed 25 ml Schlenk tube, compound **Br1a** (693 mg, 1.34 mmol, 1 eq) and *p*-tolylmercaptane (273 μ l, 2.02 mmol, 1.5 eq) were dissolved in 7 ml dry, degassed THF. NaH (60 % dispersed in mineral oil, 268.4 mg, 6.7 mmol, 5 eq) was added to the solution which was then allowed to stir at room temperature for 15 hours. The reaction mixture was quenched with water, then extracted three times with TBME, washed once with brine, dried over MgSO₄ and the solvent removed *in vacuo*. The crude product was subjected to column chromatography (*c*-hexane 4:1 DCM) to yield a pale solid (698 mg, 91 %).

¹H-NMR (400 MHz, Chloroform-d): δ = 7.50 – 7.45 (m, 6H), 7.33 – 7.07 (m, 14H), 6.98 (d, *J* = 1.8 Hz, 1H), 6.88 (d, *J* = 1.7 Hz, 1H), 3.52 (d, *J* = 2.9 Hz, 4H), 3.31 (s, 2H), 2.32 (s, 3H), 1.27 (s, 9H).

¹³C-NMR (101 MHz, Chloroform-d): δ = 151.51, 144.83, 137.99, 136.49, 135.11, 129.16, 127.98, 126.74, 124.93, 67.56, 37.25, 35.62, 35.27, 34.65, 31.38, 21.16.

• 1-(p-tolylmethylthiomethyl)-3-(mercapto)-5-(tert-butyl)benzene (**Br3a**)



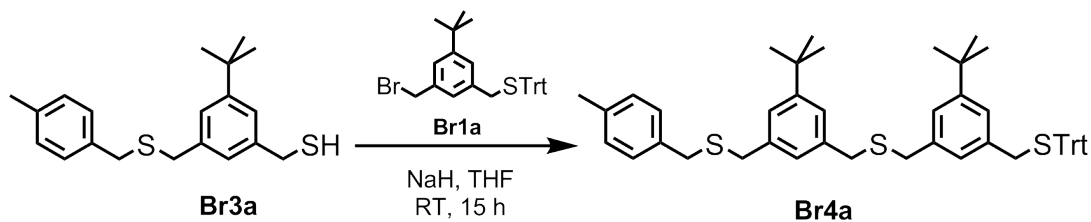
In a dry, degassed 10 ml Schlenk tube, precursor **Br2a** (698 mg, 1.22 mmol, 1 eq) was dissolved in 6 ml dry DCM, and was bubbled with argon for 15 minutes. Triethylsilane (590 μl , 3.66 mmol, 3 eq) and trifluoroacetic acid (240 μl , 4 % of DCM volume) were added to the solution. An immediate color change to yellow, fading after 5 minutes was observed. The mixture was stirred for another hour at room temperature before quenching upon addition of saturated aqueous sodium bicarbonate. The aqueous phase was extracted three times with TBME and the combined organic phase was washed once with brine, dried over MgSO_4 and the solvent removed *in vacuo*. The crude product was subjected to column chromatography (c-hexane 8:1 DCM) to yield a colorless oil (368 mg, 91 %).

$^1\text{H-NMR}$ (400 MHz, Chloroform-d): $\delta = 7.21 - 7.10$ (m, 6H), 7.07 (t, $J = 1.6$ Hz, 1H), 3.72 (d, $J = 7.5$ Hz, 2H), 3.57 (s, 4H), 2.33 (s, 3H), 1.76 (t, $J = 7.5$ Hz, 1H), 1.31 (s, 9H).

$^{13}\text{C-NMR}$ (101 MHz, Chloroform-d): $\delta = 151.78, 140.92, 138.26, 136.60, 135.08, 129.18, 128.95, 125.88, 125.00, 123.73, 35.73, 35.46, 34.73, 31.39, 29.18, 21.16$.

MALDI-TOF 331.2 (100 %), 332.3 (87 %), 333.2 (77 %).

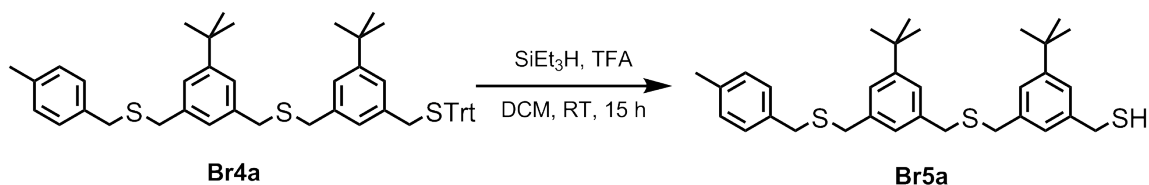
• Dimeric Branch A precursor 4 (Br4a)



In a dry, degassed 10 ml Schlenk tube, branch precursor **Br3a** (56.2 mg, 0.17 mmol, 1 eq) and branch precursor **Br1a** (87.4 mg, 0.17 mmol, 1 eq) were dissolved in 3 ml dry THF, and bubbled with argon for 15 minutes. NaH (60 % dispersion in mineral oil, 17.1 mg, 0.428 mmol, 7.4 eq) was added to the mixture which was then stirred for 15 hours at room temperature, and then quenched by addition of water. The aqueous phase was extracted three times with TBME, and the combined organic fraction was washed three times with water, dried over MgSO₄ and the solvent was removed *in vacuo*. The crude product was subjected to column chromatography (c-hexane 4:1 DCM) to afford a pale yellowish solid (102.8 mg, 79 %).

¹H-NMR (400 MHz, Chloroform-d): δ = 7.53 – 7.41 (m, 6H), 7.36 – 7.01 (m, 17H), 6.99 (s, 1H), 6.91 (s, 1H), 3.55 (d, J = 2.2 Hz, 8H), 3.31 (s, 2H), 2.31 (s, 3H), 1.30 (s, 9H), 1.27 (s, 9H).

• Dimeric Branch A (Br5a)



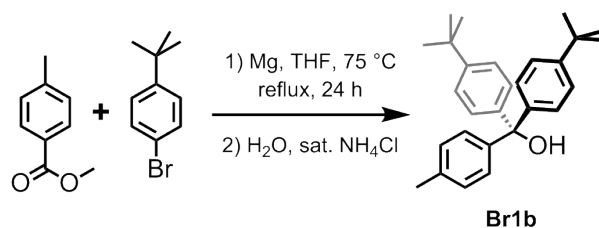
In a dry, degassed 15 ml three-neck flask, dimeric branch precursor **Br4a** (102.8 mg, 0.134 mmol, 1 eq) was dissolved in 5 ml dry DCM and bubbled with argon for 15 minutes, then triethylsilane (200 μ l, 1.255 mmol, 9.4 eq) and trifluoroacetic acid (200 μ l, 4 % of DCM volume) were added to the mixture. The reaction mixture was allowed to stir at room temperature for 15 hours, then quenched by addition of saturated aqueous sodium bicarbonate. The aqueous phase was extracted three times with DCM, dried over MgSO_4 and the solvent was removed *in vacuo*. The crude product was subjected to column chromatography (c-hexane 3:1 DCM) to afford a colorless oil (51.5 mg, 73 %).

$^1\text{H-NMR}$ (400 MHz, Chloroform-d): δ = 7.20 (dt, J = 3.4, 1.7 Hz, 4H), 7.17 – 7.11 (m, 4H), 7.11 – 7.06 (m, 2H), 3.72 (d, J = 7.5 Hz, 2H), 3.61 – 3.57 (m, 8H), 2.34 (s, 3H), 1.77 (t, J = 7.5 Hz, 1H), 1.32 (s, 2H), 1.32 (s, 9H).

MALDI-TOF 521.2 (100 %), 522.2 (56 %), 523.2 (55 %), 524.2 (36 %).

5.2.5 Branch B

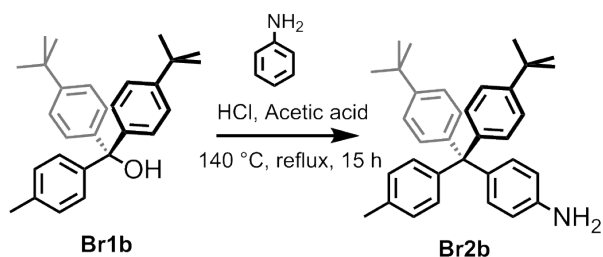
- Bis(4-(tert-butyl)phenyl)-(p-tolyl)methanol (Br1b)⁷²



In a dry degassed 500 ml two-neck flask equipped with rubber septum, reflux condenser and addition funnel, Mg turnings (4.0 g, 166.7 mmol, 2.5 eq) were suspended in 100 ml dry degassed THF under argon atmosphere. 1-bromo-4-*tert*-butylbenzene (29.1 ml, 166.7 mmol, 2.5 eq) dissolved in 100 ml dry degassed THF was added drop-wise. In order to activate the *Grignard* reagent, one pellet of iodine was added to the mixture, which was subsequently stirred for three hours. Methyl *p*-toluate (10 g, 66.7 mmol, 1 eq) was dissolved in 100 ml dry degassed THF and was added to the mixture, which was then allowed to stir at 75 °C for 24 hours. After cooling to room temperature, saturated aqueous NH₄Cl and water were added. The aqueous phase was extracted three times with Et₂O. The combined organic phases were washed twice with water, dried over MgSO₄ and the solvent was evaporated. The crude product was subjected to column chromatography (DCM 1:1 *n*-hexane) to obtain a white solid (20.2 g; 78 %).

¹H-NMR (400 MHz, Chloroform-d): δ = 7.33 – 7.28 (m, 4H), 7.20 – 7.16 (m, 6H), 7.13 – 7.09 (m, 2H), 2.70 (s, 1H), 2.34 (s, 3H), 1.30 (s, 18H).

• 4-(bis(4-(tert-butyl)phenyl)-(p-tolyl)methyl)aniline (**Br2b**)

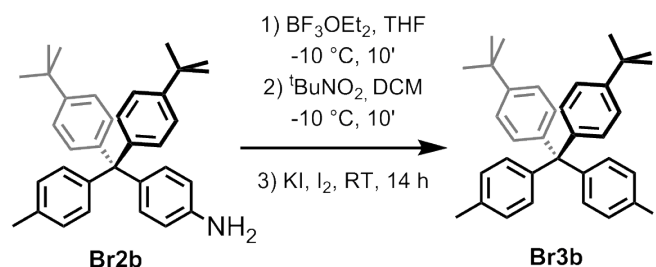


To a solution of distilled aniline (22.7 ml, 248.6 mmol, 4.75 eq) and conc. HCl (21 ml) in 150 ml glacial acetic acid in a 500 ml two-neck flask, precursor **Br1b** (20.1 g, 52.3 mmol, 1 eq) was added portionwise. The reaction mixture was refluxed and stirred at 140 °C for 15 hours. After cooling to room temperature, the acetic acid was evaporated. The solid was dissolved in DCM, washed four times with H₂O, dried over MgSO₄ and the solvent evaporated. The crude product was subjected to column chromatography (c-hexane 5:1 EtOAc and 1 % Et₃N) to afford a white solid (15.3 g; 64 %).

¹H-NMR (400 MHz, Chloroform-d): δ = 7.21 (d, *J* = 8.6 Hz, 4H), 7.11 – 7.06 (m, 6H), 7.05 – 7.01 (m, 2H), 6.96 (d, *J* = 8.6 Hz, 2H), 6.56 (d, *J* = 8.6 Hz, 2H), 2.31 (s, 3H), 2.34 (s, 3H), 1.29 (s, 18H).

GC/MS 462.2 (16 %), 461.2 (40 %), 371.2 (16 %), 370.2 (55 %), 329.1 (29 %), 328.1 (100 %), 206.95 (16 %), 57.05 (11 %).

• 4-(bis(4-(tert-butyl)phenyl)-(p-tolyl)-methyl)iodobenzene (**Br3b**)



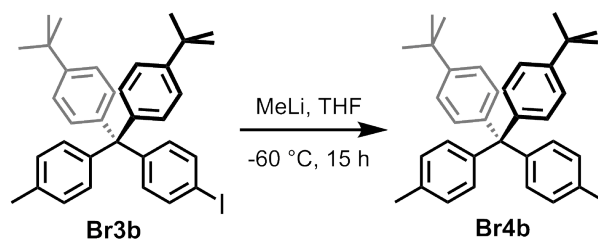
To a dry, degassed 1 L three-neck flask equipped with thermometer and rubber septa, BF_3OEt_2 (8.23 ml, 65 mmol, 2 eq) was added and the flask was cooled to -10 °C. Compound **Br2b** (15 g, 32.5 mmol, 1 eq) dissolved in 200 ml dry, degassed DCM was added dropwise. ${}^t\text{BuNO}_2$ (7.58 ml, 56.9 mmol, 1.75 eq) was dissolved in 200 ml dry, degassed THF and added dropwise. The mixture was allowed to stir for 10 minutes. KI (8 g, 48.7 mmol, 1.5 eq) and I_2 (10.9 g, 42.2 mmol, 1.3 eq) were added to the mixture. The reaction mixture was allowed to gradually warm up to room temperature and was then stirred for 15 hours at which then quenched with saturated aqueous $\text{Na}_2\text{S}_2\text{O}_3$. A pale solid precipitated which was filtered through hyflo, and redissolved in DCM. The organic phase was washed three times with water, dried over MgSO_4 and the solvent was removed *in vacuo*. The crude product was subjected to column chromatography (c-hexane) to afford pale yellowish solid (13.8 g; 74 %).

${}^1\text{H-NMR}$ (400 MHz, Chloroform-d): $\delta = 7.54$ (d, $J = 8.6$ Hz, 2H), 7.23 (d, $J = 8.6$ Hz, 4H), 7.10 – 7.03 (m, 8H), 6.96 (d, $J = 8.6$ Hz, 2H), 2.31 (s, 3H), 1.29 (s, 18H).

${}^{13}\text{C-NMR}$ (101 MHz, Chloroform-d): $\delta = 148.60$, 147.34, 143.68, 143.38, 136.35, 135.41, 133.28, 130.93, 130.58, 128.16, 124.32, 91.50, 63.58, 34.34, 31.39, 20.96.

GC/MS 573.1 (16 %), 572.05 (38 %), 515 (16 %), 482.05 (17 %), 481.05 (56 %), 445.2 (14 %), 440.05 (26 %), 439 (98 %), 370.2 (32 %), 369.2 (100 %), 207 (18 %), 57.05 (91 %).

• **Bis(4-(tert-butyl)phenyl)-bis(p-tolyl)methane (Br4b)**



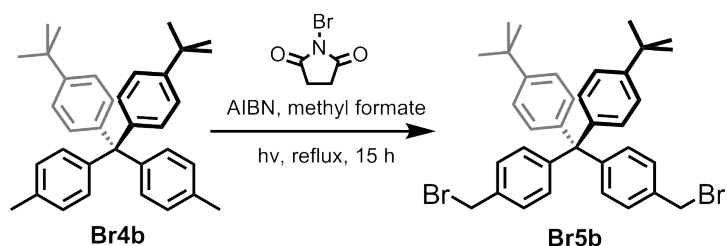
Under inert atmosphere, precursor **Br3b** (16 g, 27.9 mmol, 1 eq) was dissolved in 250 ml dry, degassed THF. The solution was cooled to -60 °C and MeLi (1.6 M solution in hexane, 52.3 ml, 83.8 mmol, 3 eq) was added dropwise. The mixture was allowed to slowly warm up to room temperature, and was stirred for 15 hours. The reaction mixture was quenched upon addition of water, extracted three times with DCM and dried over MgSO₄. The volatile was evaporated by rotavapor to afford a white solid (11,6 g, 90 %).

¹H-NMR (400 MHz, Chloroform-d): δ = 7.23 – 7.21 (m, 4H), 7.11 – 7.06 (m, 8H), 7.03 (d, J = 8.3 Hz, 4H), 2.31 (s, 6H), 1.29 (d, J = 1.1 Hz, 18H).

¹³C-NMR (101 MHz, Chloroform-d): δ = 148.25, 144.40, 144.08, 135.06, 131.06, 130.68, 127.96, 124.11, 63.46, 34.30, 31.39, 20.95.

GC/MS 461.2 (10 %), 460.25 (30 %), 403.2 (17 %), 370.2 (33 %), 369.2 (87 %), 328.15 (25 %), 327.15 (100 %), 297.1 (10 %), 215.1 (23 %), 207 (11 %) 179.05 (10 %), 57.1 (44 %).

• **Di-(4-(tert-butyl)phenyl)-bis(4-(bromomethyl)phenyl)methane (Br5b)**

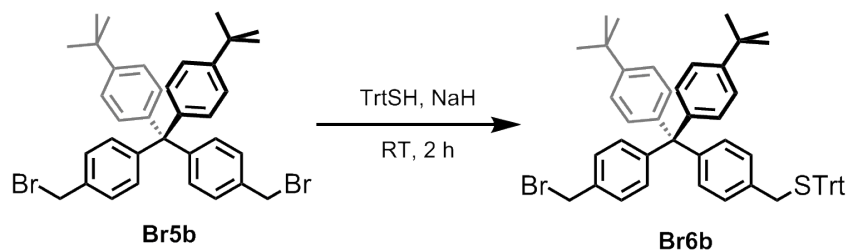


In a dry, degassed 500 ml two-neck flask equipped with a reflux condenser and a glass stopper, **Br4b** (5 g, 10.9 mmol, 1 eq), **NBS** (7.8 g, 43.4 mmol, 4 eq) and catalytic amounts of **AIBN** (180 mg, radical starter) were suspended in 150 ml methyl formate under inert atmosphere. The reaction was activated by illumination with a 500 W halogen lamp and refluxed for 15 hours, then cooled to room temperature. The solvent was evaporated, and the residue dissolved in DCM. The mixture was washed four times with water and dried over MgSO_4 . The volatile was evaporated and the crude product subjected to column chromatography (c-hexane 20:1 DCM) to afford a white solid (4.0 g, 60 %).

$^1\text{H-NMR}$ (400 MHz, Chloroform-d): $\delta = 7.28 - 7.27$ (m, 2H), 7.25 (s, 6H), 7.23 (d, $J = 2.0$ Hz, 2H), 7.20 – 7.16 (m, 2H), 7.10 – 7.05 (m, 4H), 4.48 (s, 4H), 1.30 (s, 18H).

$^{13}\text{C-NMR}$ (101 MHz, Chloroform-d): $\delta = 148.73, 147.35, 143.15, 135.16, 131.49, 130.60, 128.12, 124.40, 63.86, 34.35, 33.47, 31.38$.

- **Bis(4-(tert-butyl)phenyl)-(4-(bromomethyl)phenyl)-(4-trithylthiomethylphenyl)-methane (Br6b)**



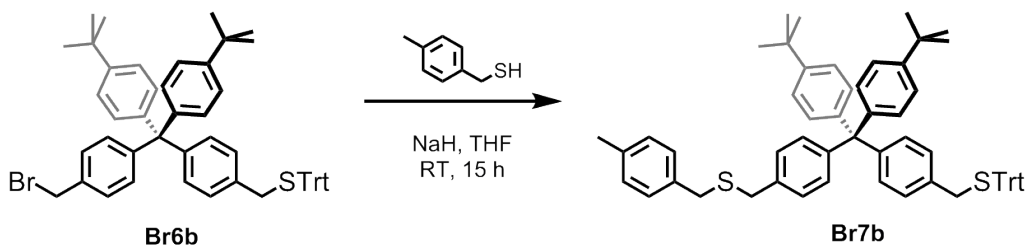
Compound **Br5b** (100 mg, 0.162 mmol, 1 eq) was dissolved in 5 ml dry THF in a 10 ml Schlenk tube. Trithylthiol (27.6 mg, 0.097 mmol, 0.6 eq) was added to the solution which was then bubbled for 30 minutes. NaH (60 % dispersion in mineral oil, 2 eq) was added to the flask. The mixture was stirred at room temperature for 15 hours, and then quenched by addition of water, extracted two times with TBME, washed twice with water, dried over MgSO₄ and the solvent was removed *in vacuo*. The crude product was subjected to column chromatography (c-hexane 2:1 DCM) to afford a pale solid (37.9, 48 %).

¹H-NMR (400 MHz, Chloroform-d): δ = 7.48 – 7.43 (m, 5H), 7.30 (s, 4H), 7.26 (d, J = 1.7 Hz, 6H), 7.24 – 7.18 (m, 7H), 7.15 (d, J = 8.4 Hz, 2H), 7.08 – 7.04 (m, 5H), 7.00 (d, J = 8.3 Hz, 2H), 4.47 (s, 2H), 3.28 (s, 2H), 1.29 (s, 18H).

¹³C-NMR (101 MHz, Chloroform-d): δ = 148.25, 144.40, 144.08, 135.06, 131.06, 130.68, 127.96, 124.11, 63.46, 34.30, 31.39, 20.95.

MALDI-TOF 811.5 (98 %), 812.6 (80 %), 813.5 (100 %), 814.7 (88 %).

- Bis(4-(tert-butyl)phenyl)-(4-(p-tolylmethylthiomethyl)phenyl)-(4-triethylthiomethylphenyl)-methane (**Br7b**)



To a dry, degassed 5 ml Schlenk tube, compound **Br6b** (100 mg, 0.123 mmol, 1 eq) was added and dissolved in 2 ml dry THF. *p*-tolylmercaptane (25 μ l, 0.185 mmol, 1.5 eq) was added to the solution which was then bubbled for 15 minutes. NaH (60% dispersed in mineral oil, 24.6 mg, 0.615 mmol, 5 eq) was added to the reaction mixture. The mixture was stirred at room temperature for 15 hours, and then quenched by addition of water, extracted two times with TBME, washed twice with water, dried over MgSO₄ and the solvent was removed *in vacuo*. The crude product was subjected to column chromatography (c-hexane 4:1 DCM) to afford a pale, yellowish solid (91 mg, 85 %).

¹H-NMR (400 MHz, Chloroform-d): δ = 7.48 – 7.42 (m, 6H), 7.30 – 6.98 (m, 29H), 3.56 (d, *J* = 10.5 Hz, 4H), 3.28 (s, 2H), 2.31 (s, 3H), 1.29 (s, 18H).

¹³C-NMR (101 MHz, Chloroform-d): δ = 148.45, 146.00, 145.85, 144.73, 143.66, 136.55, 135.52, 135.13, 134.33, 131.24, 130.67, 129.66, 129.16, 128.91, 128.10, 127.94, 126.70, 124.21, 67.42, 63.69, 36.66, 35.49, 35.23, 34.33, 31.40, 29.74, 21.14.

MALDI-TOF 869.4 (100 %), 870.5 (97 %), 871.6 (93 %).

- Bis(4-(tert-butyl)phenyl)-(4-(p-tolylmethylthiomethyl)phenyl)-(4-mercaptophenyl)-methane (**Br8b**)

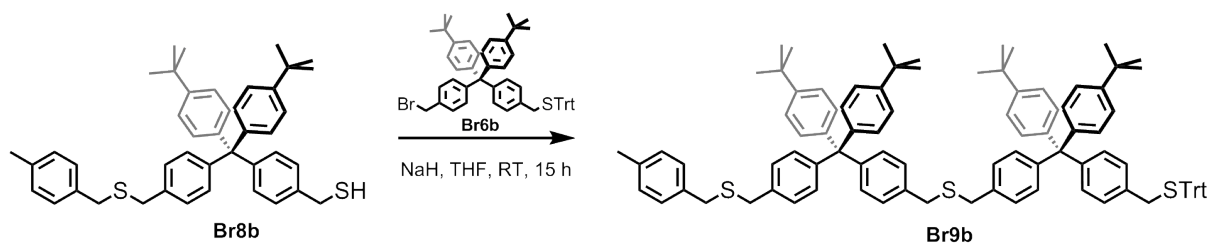


In a dry, degassed 10 ml Schlenk tube, branch precursor **Br7b** (91 mg, 0.104 mmol, 1 eq) was dissolved in 2 ml dry DCM, and bubbled with argon for 20 minutes. Triethylsilane (150.9 μ l, 0.936 mmol, 9 eq) and trifluoroacetic acid (80 μ l, 4 % of DCM volume) were added to the mixture. An immediate color change to yellow, lasting for 30 seconds was observed. The mixture was stirred 1 more hour at room temperature, and then quenched by addition of saturated aqueous sodium bicarbonate. The aqueous phase was extracted three times with DCM, dried over MgSO_4 and the solvent was removed *in vacuo*. The crude product was subjected to column chromatography (c-hexane 8:1 DCM) to afford a colorless oil (65.6 mg, quant.).

$^1\text{H-NMR}$ (400 MHz, Chloroform-d): δ = 7.25 – 7.07 (m, 21H), 3.70 (d, J = 7.5 Hz, 2H), 3.57 (d, J = 9.8 Hz, 4H), 2.31 (s, 3H), 1.75 (t, J = 7.5 Hz, 1H), 1.30 (s, 18H).

$^{13}\text{C-NMR}$ (101 MHz, Chloroform-d): δ = 148.54, 146.06, 145.84, 143.65, 138.40, 136.57, 135.62, 135.14, 131.47, 131.28, 130.72, 129.18, 128.93, 127.98, 127.00, 124.27, 63.72, 35.54, 35.26, 34.36, 31.43, 28.58, 21.17.

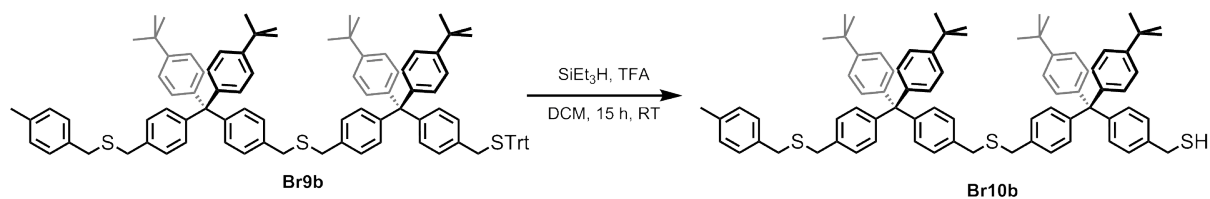
• Dimeric Branch B Precursor (**Br9b**)



In a dry, degassed 10 ml Schlenk tube, branch precursor **Br8b** (35 mg, 0.057 mmol, 1 eq) and branch precursor **Br6b** (57.1 mg, 0.07 mmol, 1.2 eq) were dissolved in 3 ml dry THF, and bubbled with argon for 15 minutes. NaH (60 % dispersion in mineral oil, 17.1 mg, 0.428, 7.4 eq) was added to the mixture which was then stirred for 15 hours at room temperature, and then quenched by addition of water. The mixture was extracted three times with TBME, washed three times with water, dried over MgSO_4 and the solvent was removed *in vacuo*. The crude product was subjected to column chromatography (c-hexane 4:1 DCM and c-hexane 1:1 DCM) to afford a pale yellowish solid (56.9 mg, 74 %).

$^1\text{H-NMR}$ (400 MHz, Chloroform- d): δ = 7.48 – 7.43 (m, 6H), 7.30 – 7.17 (m, 16H), 7.16 – 7.04 (m, 27H), 7.02 – 6.98 (m, 2H), 3.61 – 3.55 (m, 8H), 3.27 (s, 2H), 2.31 (s, 3H), 1.29 (s, 18H), 1.28 (s, 18H).

• Dimeric Branch B (Br10b)



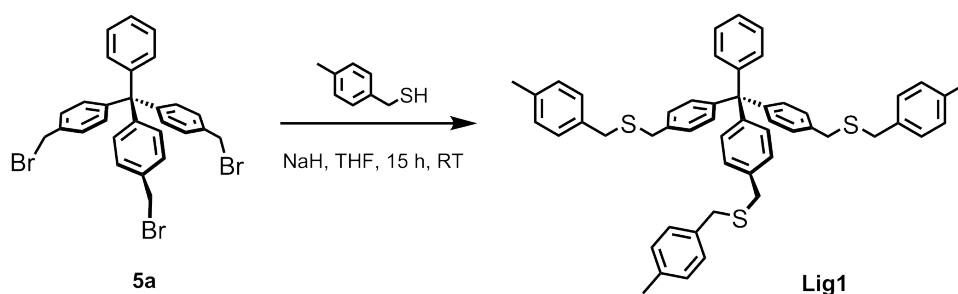
In a dry, degassed 10 ml two-neck flask, dimeric branch precursor **Br4b** (56.9 mg, 0.042 mmol, 1 eq) was dissolved in 3 ml dry DCM, and bubbled with argon for 15 minutes, then triethylsilane (200 μl , 1.255 mmol, 30 eq) and trifluoroacetic acid (120 μl , 4 % of DCM volume) were added. The reaction mixture was allowed to stir at room temperature for 15 hours, and then quenched by addition of saturated aqueous sodium bicarbonate. The mixture phase was extracted three times with DCM, washed twice with water, dried over MgSO_4 and the solvent was removed *in vacuo*. The crude product was subjected to column chromatography (c-hexane 3:1 DCM) to afford a pale solid (20.6 mg, 44 %).

$^1\text{H-NMR}$ (400 MHz, Chloroform- d): δ = 7.26 – 7.20 (m, 8H), 7.17 – 7.05 (m, 28H), 3.71 (d, J = 7.5 Hz, 2H), 3.61 – 3.55 (m, 8H), 2.32 (s, 3H), 1.75 (t, J = 7.5 Hz, 1H), 1.29 (s, 18H), 1.29 (s, 18H).

MALDI-TOF 1117.7 (100 %), 1118.8 (97 %), 1119.8 (85 %), 1120.7 (74 %).

5.2.6 Ligands

• Gold Nanoparticle Ligand 1 (Lig1)



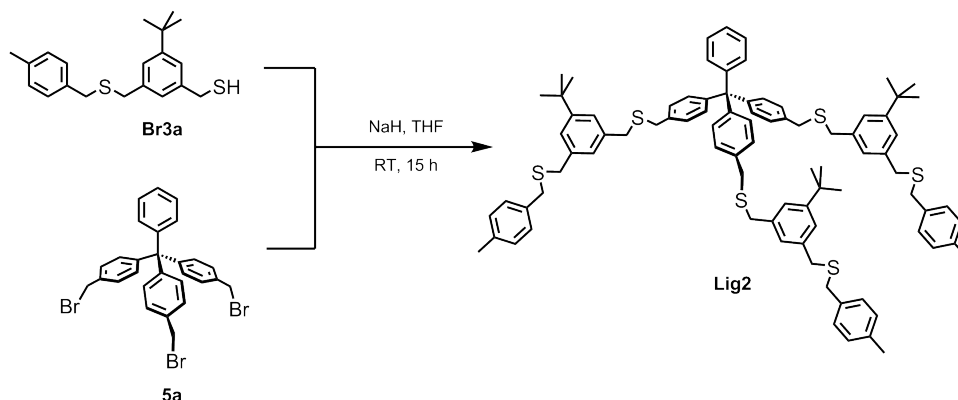
In a dry, degassed 15 ml two-neck flask, precursor **5a** (52.4 mg, 0.087 mmol, 1 eq) and *p*-tolylmercaptane (71.1 μ l, 0.53 mmol, 6 eq) were dissolved in 5 ml dry THF. After bubbling with argon for 15 minutes, NaH (60 % dispersed in mineral oil, 35 mg, 0.87 mmol, 10 eq) was added. The mixture was allowed to stir at room temperature for 15 hours, and was then quenched upon addition of water. The aqueous phase was extracted three times with TBME. The combined organic phases were washed three times with water, dried over MgSO₄, and evaporated to dryness. The product was afforded by column chromatography (c-hexane 5:1 DCM, and c-hexane 3:2 DCM) as a yellowish oil (61.9 mg, 92 %).

¹H-NMR (400 MHz, Chloroform-d): δ = 7.25 – 7.06 (m, 29H), 3.58 (d, J = 11.6 Hz, 12H), 2.31 (s, 9H).

¹³C-NMR (101 MHz, Chloroform-d): δ = 146.72, 145.47, 136.61, 135.85, 135.07, 131.19, 131.08, 129.19, 128.91, 128.14, 127.53, 126.00, 64.32, 35.60, 35.22, 21.15.

MALDI-TOF 769.4 (100 %), 770.4 (91 %), 771.4 (85 %), 772.4 (76 %), 773.4 (72 %).

• Gold Nanoparticle Ligand 2 (Lig2)

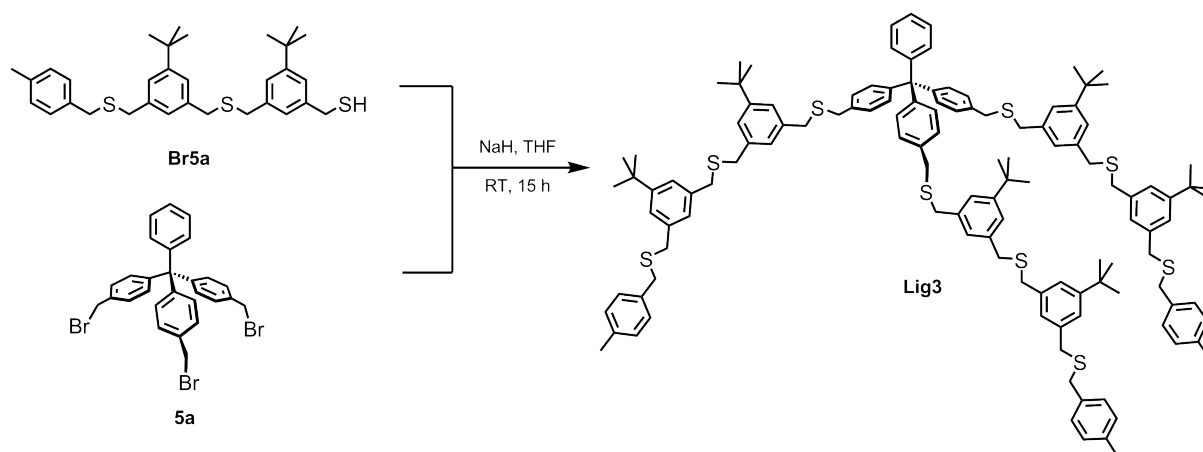


In a dry, degassed 15 ml three-neck flask, precursor **5a** (51.8 mg, 0.086 mmol, 1 eq) and branch **Br3a** (141.5 mg, 0.43 mol, 5 eq) were dissolved in 5 ml dry THF. After bubbling with argon for 15 minutes, NaH (60 % dispersed in mineral oil, 34.6 mg, 0.86 mmol, 10 eq) was added. The mixture was allowed to stir at room temperature for 15 hours, and was then quenched upon addition of water. The aqueous phase was extracted three times with TBME. The combined organic phases were washed three times with water, dried over MgSO₄, and evaporated to dryness. The product was afforded after column chromatography (*c*-hexane 5:2 DCM and *c*-hexane 1:1 DCM) and automated GPC (chloroform) as a yellowish oil (83.3 mg, 72 %).

¹H-NMR (400 MHz, Chloroform-d): δ = 7.23 – 7.06 (m, 38H), 3.59 (d, *J* = 14.4 Hz, 12H), 3.55 (d, *J* = 3.8 Hz, 12H), 2.31 (s, 9H), 1.29 (s, 27H).

¹³C-NMR (101 MHz, Chloroform-d): δ = 151.48, 146.72, 145.51, 138.07, 137.89, 136.56, 135.73, 135.10, 131.21, 131.07, 129.18, 128.95, 128.19, 127.57, 126.83, 126.02, 124.92, 124.81, 64.35, 36.17, 35.79, 35.43, 35.29, 34.68, 31.42, 21.17.

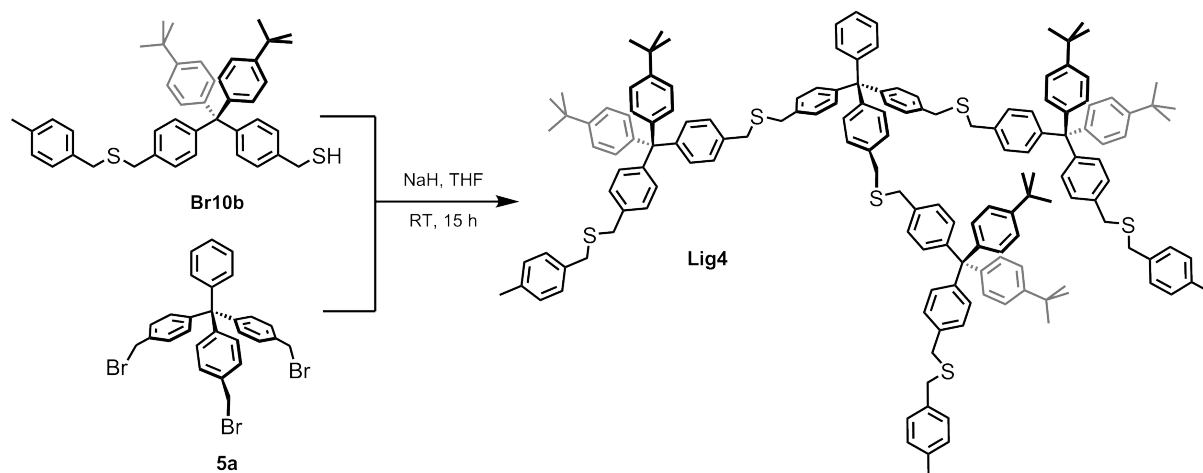
• Gold Nanoparticle Ligand 3 (Lig3)



In a dry, degassed 15 ml three-neck flask, tripodal precursor **5a** (15.9 mg, 0.026 mmol, 1 eq) and branch **Br5a** (54.4 mg, 0.104 mol, 4 eq) were dissolved in 3 ml dry THF. After bubbling with argon for 15 minutes, NaH (60 % dispersed in mineral oil, 15.9 mg, 0.398 mmol, 15.3 eq) was added. The mixture was allowed to stir at room temperature for 15 hours, and was then quenched upon addition of water. The aqueous phase was extracted three times with TBME. The combined organic phases were washed twice with water, dried over MgSO_4 , and evaporated to dryness. The crude product was subjected to plaque filtration (c-hexane 1:1 DCM), and was purified by automated GPC (chloroform) thereafter to recover a yellowish oil (5.7 mg, 11 %).

$^1\text{H-NMR}$ (400 MHz, Chloroform-d): $\delta = 7.22 - 7.12$ (m, 35H), $7.11 - 7.08$ (m, 9H), 7.06 (s, 3H), 3.62 (s, 6H), $3.59 - 3.55$ (m, 30H), 2.32 (s, 9H), 1.30 (s, 27H), 1.29 (s, 27H).

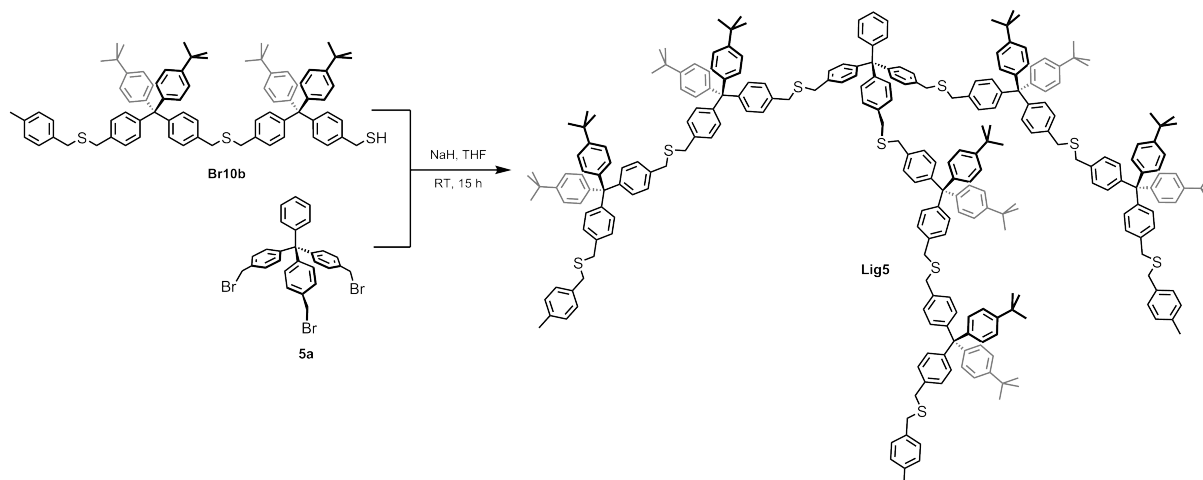
• Gold Nanoparticle Ligand 4 (Lig4)



In a dry, degassed 10 ml Schlenk tube, tripodal precursor **5a** (7.2 mg, 0.012 mmol, 1 eq) and branch **Br8b** (35 mg, 0.057 mol, 4.7 eq) were dissolved in 5 ml dry THF. After bubbling with argon for 15 minutes, NaH (60 % dispersed in mineral oil, 7.2 mg, 0.18 mmol, 15 eq) was added. The mixture was allowed to stir at room temperature for 15 hours, and was then quenched upon addition of water. The aqueous phase was extracted three times with TBME. The combined organic phases were washed three times with water, dried over MgSO₄, and evaporated to dryness. The product was afforded by automated GPC (chloroform) as a yellowish oil (14.4 mg, 25 %).

¹H-NMR (400 MHz, Chloroform-d): δ = 7.22 – 7.12 (m, 35H), 7.11 – 7.08 (m, 9H), 7.06 (s, 3H), 3.62 (s, 6H), 3.59 – 3.55 (m, 30H), 2.32 (s, 9H), 1.30 (s, 27H), 1.29 (s, 27H).

• Gold Nanoparticle Ligand 5 (Lig5)

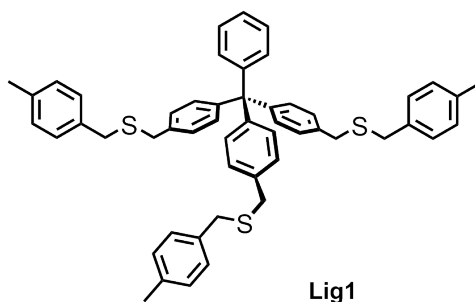


In a dry, degassed 15 ml three-neck flask, tripodal precursor **5a** (15.9 mg, 0.026 mmol, 1 eq) and branch **Br5a** (54.4 mg, 0.104 mol, 4 eq) were dissolved in 3 ml dry THF. After bubbling with argon for 15 minutes, NaH (60 % dispersed in mineral oil, 15.9 mg, 0.398 mmol, 15.3 eq) was added. The mixture was allowed to stir at room temperature for 15 hours, and was then quenched upon addition of water. The aqueous phase was extracted three times with TBME. The combined organic phases were washed twice with water, dried over MgSO₄, and evaporated to dryness. The crude product was subjected to plaque filtration (c-hexane 1:1 DCM), and was purified by automated GPC (chloroform) thereafter to recover a yellowish oil (6.0 mg, 40 %).

¹H-NMR (400 MHz, Chloroform-d): δ = 7.25 – 7.16 (m, 35H), 7.14 – 7.11 (m, 57H), 7.09 – 7.04 (m, 33H), 3.60 – 3.54 (m, 36H), 2.31 (s, 9H), 1.28 (s, 54H), 1.27 (s, 54H).

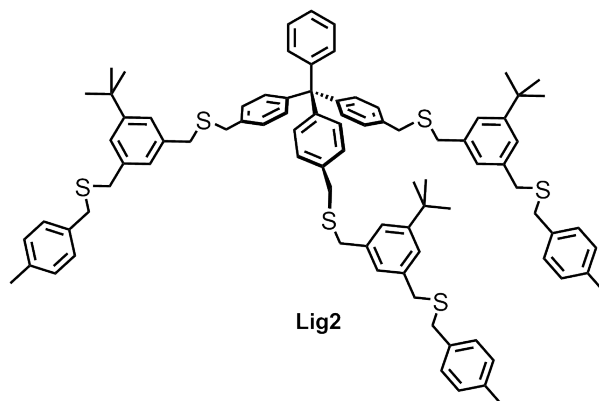
5.2.7 Gold Nanoparticles

- Gold Nanoparticle from Lig1 (Au-Lig1)



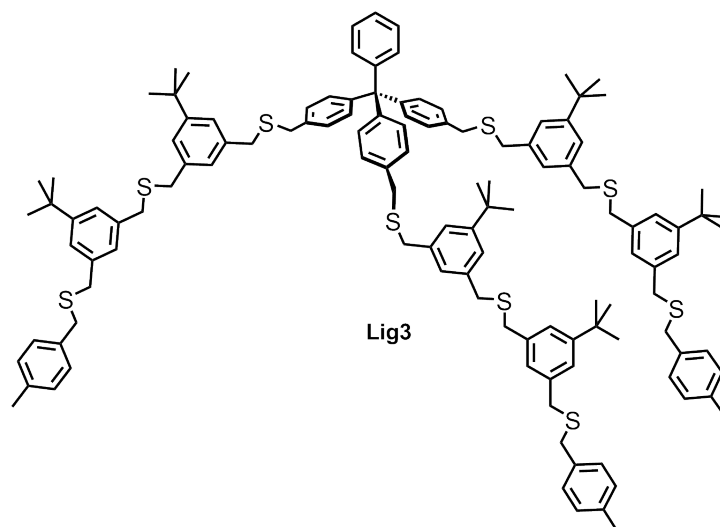
To a 50 ml 1-neck flask containing a solution of HAuCl_4 (29.0 mg, 0.085 mmol, 3.3 eq) in 2 ml deionized water, a solution of TOAB (85.3 mg, 0.156 mmol, 6 eq) in 2 ml DCM was added. After stirring the biphasic system for 15 minutes at room temperature, the aqueous phase had turned colorless, while the organic phase had acquired an orange color. **Lig1** (20.2 mg, 0.026 mmol, 1 eq) dissolved in 2 ml DCM was added, and the mixture was allowed to stir at room temperature. After 15 minutes, a solution of NaBH_4 (23.7 mg, 0.627, 24 eq) in 2 ml water was added at once, initiating gas formation and an immediate color change to dark brown. After stirring the mixture for 15 more minutes, the organic phase was transferred to a falcon tube via pasteur pipette, and the solution slowly concentrated by a steady argon stream until approximately 0.5 ml of solvent remained. Fast addition of approximately 40 ml of EtOH induced the precipitation of the dark brown crude product. The mixture was centrifuged at 4000 rpm and 5 °C for 25 minutes, and then cautiously decanted. The dark brown residue had changed to an even darker shade. Again 40 ml of EtOH were added, and the centrifuge and decanting procedure repeated twice more. Trying to redissolve the particles in DCM failed. Also the purification of the crude particles by manual GPC could not be accomplished.

- Gold Nanoparticle from Lig2 (Au-Lig2)



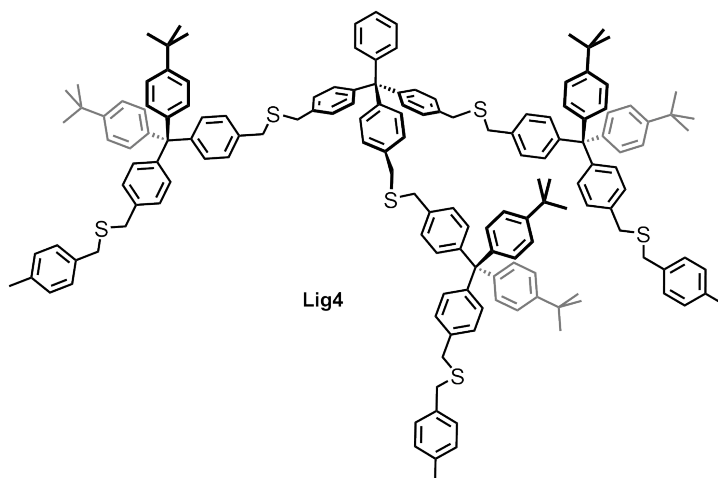
To a 50 ml 1-neck flask containing a solution of HAuCl_4 (31.4 mg, 0.092 mmol, 6.2 eq) in 2 ml deionized water, a solution of TOAB (97.5 mg, 0.178 mmol, 11.9 eq) in 2 ml DCM was added. After stirring the biphasic system for 15 minutes at room temperature, the aqueous phase had turned colorless, while the organic phase had acquired an orange color. **Lig2** (20.1 mg, 0.015 mmol, 1 eq) dissolved in 2 ml DCM was added, and the mixture was allowed to stir at room temperature. After 15 minutes, a solution of NaBH_4 (27 mg, 0.714, 47.6 eq) in 2 ml water was added at once, initiating gas formation and an immediate color change to dark brown. After stirring the mixture for 15 more minutes, the organic phase was transferred to a falcon tube via pasteur pipette, and the solution slowly concentrated by a steady argon stream until approximately 0.5 ml of solvent remained. Fast addition of approximately 40 ml of EtOH induced the precipitation of the dark brown crude product. The mixture was centrifuged at 4000 rpm and 5 °C for 25 minutes, and then cautiously decanted. The dark brown residue had changed to an even darker shade. Again 40 ml of EtOH were added, and the centrifuge and decanting procedure repeated twice more. Trying to redissolve the particles in DCM failed. Also the purification of the crude particles by manual GPC could not be accomplished.

• Gold Nanoparticle from Lig3 (Au-Lig3)



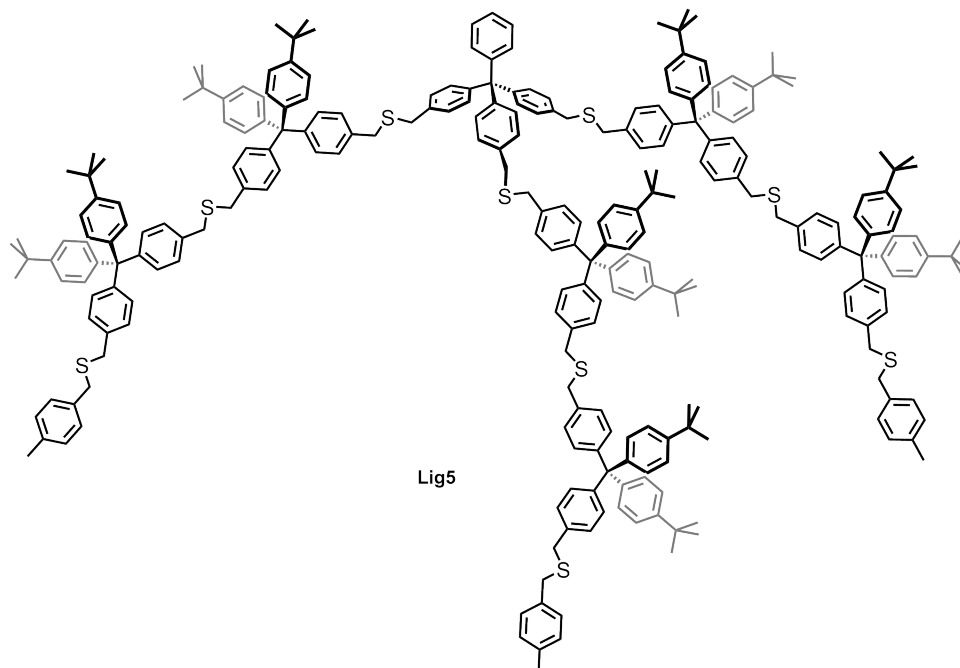
To a 25 ml 1-neck flask containing a solution of HAuCl_4 (9.6 mg, 0.028 mmol, 9.3 eq) in 2 ml deionized water, a solution of TOAB (29.4 mg, 0.178 mmol, 17.9 eq) in 2 ml DCM was added. After stirring the biphasic system for 15 minutes at room temperature, the aqueous phase had turned colorless, while the organic phase had acquired an orange color. **Lig3** (5.7 mg, 0.003 mmol, 1 eq) dissolved in 2 ml DCM was added, and the mixture was allowed to stir at room temperature. After 15 minutes, a solution of NaBH_4 (8.7 mg, 0.23 mmol, 76.7 eq) in 2 ml water was added at once, initiating gas formation and an immediate color change to dark brown. After stirring the mixture for 15 more minutes, the organic phase was transferred to a falcon tube via pasteur pipette, and the solution slowly concentrated by a steady argon stream until approximately 0.5 ml of solvent remained. Fast addition of approximately 40 ml of EtOH induced the precipitation of the dark brown crude product. The mixture was centrifuged at 4000 rpm and 5 °C for 25 minutes, and then cautiously decanted. The dark brown residue had changed to an even darker shade. Again 40 ml of EtOH were added, and the centrifuge and decanting procedure repeated twice more. The particles were subjected to manual GPC (DCM) and collected in small fractions. UV/Vis absorption measurements allowed to separate pure particles from fractions containing excess amounts of ligands. The dissolved pure particles were thereafter evaporated to dryness *in vacuo* at 30 °C, yielding a brown waxy solid (2.1 mg, 26 % with respect to gold).

• Gold Nanoparticle from Lig4 (Au-Lig4)



To a 25 ml 1-neck flask containing a solution of HAuCl₄ (14.7 mg, 0.043 mmol, 6.6 eq) in 2 ml deionized water, a solution of TOAB (42.4 mg, 0.077 mmol, 12 eq) in 2 ml DCM was added. After stirring the biphasic system for 15 minutes at room temperature, the aqueous phase had turned colorless, while the organic phase had acquired an orange color. **Lig4** (14.4 mg, 0.0064 mmol, 1 eq) dissolved in 2 ml DCM was added, and the mixture was allowed to stir at room temperature. After 15 minutes, a solution of NaBH₄ (12.1 mg, 0.381, 59.5 eq) in 2 ml water was added at once, initiating gas formation and an immediate color change to dark brown. After stirring the mixture for 15 more minutes, the organic phase was transferred to a falcon tube via pasteur pipette, and the solution slowly concentrated by a steady argon stream until approximately 0.5 ml of solvent remained. Fast addition of approximately 40 ml of EtOH induced the precipitation of the dark brown crude product. The mixture was centrifuged at 4000 rpm and 5 °C for 25 minutes, and then cautiously decanted. The dark brown residue had changed to an even darker shade. Again 40 ml of EtOH were added, and the centrifuge and decanting procedure repeated twice more. The particles were subjected to manual GPC (DCM) and collected in small fractions. UV/Vis absorption measurements allowed to separate pure particles from fractions containing excess amounts of ligands. The dissolved pure particles were thereafter evaporated to dryness *in vacuo* at 30 °C, yielding a brown waxy solid (6.8 mg, 60 % with respect to gold).

• Gold Nanoparticle from Lig5 (Au-Lig5)



To a 25 ml 1-neck flask containing a solution of HAuCl_4 (5.2 mg, 0.015 mmol, 9.4 eq) in 2 ml deionized water, a solution of TOAB (16 mg, 0.029 mmol, 18.3 eq) in 2 ml DCM was added. After stirring the biphasic system for 15 minutes at room temperature, the aqueous phase had turned colorless, while the organic phase had acquired an orange color. **Lig5** (6 mg, 0.0016 mmol, 1 eq) dissolved in 2 ml DCM was added, and the mixture was allowed to stir at room temperature. After 15 minutes, a solution of NaBH_4 (4.6 mg, 0.122, 76.1 eq) in 2 ml water was added at once, initiating gas formation and an immediate color change to dark brown. After stirring the mixture for 15 more minutes, the organic phase was transferred to a falcon tube via pasteur pipette, and the solution slowly concentrated by a steady argon stream until approximately 0.5 ml of solvent remained. Fast addition of approximately 40 ml of EtOH induced the precipitation of the dark brown crude product. The mixture was centrifuged at 4000 rpm and 5 °C for 25 minutes, and then cautiously decanted. The dark brown residue had changed to an even darker shade. Again 40 ml of EtOH were added, and the centrifuge and decanting procedure repeated twice more. The particles were subjected to GPC (DCM) and collected in small fractions. UV/Vis absorption measurements allowed to separate pure particles from fractions containing excess amounts of ligands. The dissolved pure particles were thereafter evaporated to dryness *in vacuo* at 30 °C, yielding a brown waxy solid (4.6 mg, 72 % with respect to gold).

References

- [1] Faraday, M. *Philosophical Transactions of the Royal Society of London* **1857**, *147*, 145–181.
- [2] Zsigmondy, R. *Justus Liebigs Ann. Chem.* **1898**, *301*, 29–54.
- [3] Svedberg, T. *Ber. Dtsch. Chem. Ges.* **1906**, *39*, 1705–1714.
- [4] Svedberg, T. *Ber. Dtsch. Chem. Ges.* **1914**, *47*, 12–38.
- [5] Turkevich, J.; Stevenson, P. C.; Hillier, J. *Discuss. Faraday Soc.* **1951**, *11*, 55–75.
- [6] Brown, D. H.; Smith, W. E. *Chem. Soc. Rev.* **1980**, *9*, 217–240.
- [7] Whitesell, J. K.; Chang, H. K. *Science* **1993**, *261*, 73–76.
- [8] Giersig, M.; Mulvaney, P. *Langmuir* **1993**, *9*, 3408–3413.
- [9] Brust, M.; Walker, M.; Bethell, D.; Schiffrin, D. J.; Whyman, R. *J. Chem. Soc., Chem. Commun.* **1994**, 801–802.
- [10] Brust, M.; Fink, J.; Bethell, D.; Schiffrin, D. J.; Kiely, C. *J. Chem. Soc., Chem. Commun.* **1995**, 1655–1656.
- [11] Peng, G.; Tisch, U.; Adams, O.; Hakim, M.; Shehada, N.; Broza, Y. Y.; Billan, S.; Abdah-Bortnyak, R.; Kuten, A.; Haick, H. *Nat. Nano* **2009**, *4*, 669–673.
- [12] Daniel, M.-C.; Astruc, D. *Chem. Rev.* **2003**, *104*, 293–346.
- [13] Taton, T. A. *Trends in Biotechnology* **2002**, *20*, 277–279.
- [14] Niemeyer, C. M. *Angew. Chem. Int. Ed.* **2001**, *40*, 4128–4158.
- [15] Moores, A.; Goettmann, F. *New J. Chem.* **2006**, *30*, 1121–1132.
- [16] Stuchinskaya, T.; Moreno, M.; Cook, M. J.; Edwards, D. R.; Russell, D. A. *Photochem. Photobiol. Sci.* **2011**, *10*, 822–831.
- [17] Brown, S. D.; Nativo, P.; Smith, J.-A.; Stirling, D.; Edwards, P. R.; Venugopal, B.; Flint, D. J.; Plumb, J. A.; Graham, D.; Wheate, N. J. *J. Am. Chem. Soc.* **2010**, *132*, 4678–4684.
- [18] Kim, S.-J.; Lee, J.-S. *Nano Lett.* **2010**, *10*, 2884–2890.
- [19] Liao, J.; Bernard, L.; Langer, M.; Schönenberger, C.; Calame, M. *Adv. Mater.* **2006**, *18*, 2444–2447.
- [20] Huang, D.; Liao, F.; Moles, S.; Redinger, D.; Subramanian, V. *J. Electrochem. Soc.* **2003**, *150*, G412–G417.
- [21] Sardar, R.; Funston, A. M.; Mulvaney, P.; Murray, R. W. *Langmuir* **2009**, *25*, 13840–13851.
- [22] Homburger, M.; Simon, U. *Phil. Trans. R. Soc. A* **2010**, *368*, 1405–1453.
- [23] Schmid, G.; Simon, U. *Chem. Commun.* **2005**, 697–710.
- [24] Mangold, M. A.; Calame, M.; Mayor, M.; Holleitner, A. W. *ACS Nano* **2012**, *6*, 4181–4189.
- [25] Johnson, S. R.; Evans, S. D.; Mahon, S. W.; Ulman, A. *Langmuir* **1997**, *13*, 51–57.
- [26] Schmid, G.; Bäuml, M.; Geerkens, M.; Heim, I.; Osemann, C.; Sawitowski, T. *Chem. Soc. Rev.* **1999**, *28*, 179–185.

- [27] Alvarez, M. M.; Khoury, J. T.; Schaaff, T. G.; Shafigullin, M. N.; Vezmar, I.; Whetten, R. L. *J. Phys. Chem. B* **1997**, *101*, 3706–3712.
- [28] Wei, A. *Chem. Commun.* **2006**, 1581–1591.
- [29] Huang, X.; Li, B.; Zhang, H.; Hussain, I.; Liang, L.; Tan, B. *Nanoscale* **2011**, *3*, 1600–1607.
- [30] Giangregorio, M. M.; Losurdo, M.; Bianco, G. V.; Operamolla, A.; Dilonardo, E.; Sacchetti, A.; Capezzuto, P.; Babudri, F.; Bruno, G. *J. Phys. Chem. C* **2011**, *115*, 19520–19528.
- [31] Thompson, D. T. *Nano Today* **2007**, *2*, 40–43.
- [32] Peterle, T.; Ringler, P.; Mayor, M. *Adv. Funct. Mater.* **2009**, *19*, 3497–3506.
- [33] Peterle, T.; Leifert, A.; Timper, J.; Sologubenko, A.; Simon, U.; Mayor, M. *Chem. Commun.* **2008**, 3438–3440.
- [34] Hermes, J. P.; Sanders, F.; Peterle, T.; Urbani, R.; Pfohl, T.; Thompson, D.; Mayor, M. *Chem. Eur. J.* **2011**, *17*, 13473–13481.
- [35] Hermes, J. P.; Sanders, F.; Peterle, T.; Mayor, M. *Chimia (Aarau)* **2011**, *65*, 219–222.
- [36] Hermes, J. P.; Sander, F.; Fluch, U.; Peterle, T.; Thompson, D.; Urbani, R.; Pfohl, T.; Mayor, M. *J. Am. Chem. Soc.* **2012**, *134*, 14674–14677.
- [37] Wojczykowski, K.; Meißner, D.; Jutzi, P.; Ennen, I.; Hütten, A.; Fricke, M.; Volkmer, D. *Chem. Commun.* **2006**, 3693–3695.
- [38] Zhang, S.; Leem, G.; Srisombat, L.-o.; Lee, T. R. *J. Am. Chem. Soc.* **2007**, *130*, 113–120.
- [39] Srisombat, L.-o.; Zhang, S.; Lee, T. R. *Langmuir* **2009**, *26*, 41–46.
- [40] Wang, W.; Zhang, S.; Chinwangso, P.; Advincula, R. C.; Lee, T. R. *J. Phys. Chem. C* **2009**, *113*, 3717–3725.
- [41] Park, J.-S.; Vo, A. N.; Barriet, D.; Shon, Y.-S.; Lee, T. R. *Langmuir* **2005**, *21*, 2902–2911.
- [42] Pankau, W. M.; Verbist, K.; Kiedrowski, G. v. *Chem. Commun.* **2001**, 519–520.
- [43] Perumal, S.; Hofmann, A.; Scholz, N.; Rühl, E.; Graf, C. *Langmuir* **2011**, *27*, 4456–4464.
- [44] Sander, F.; Fluch, U.; Hermes, J. P.; Mayor, M. *Small* **2014**, *10*, 349–359.
- [45] Schmid, G. *Adv. Eng. Mater.* **2001**, *3*, 737–743.
- [46] Aikens, C. M. *J. Phys. Chem. Lett.* **2011**, *2*, 99–104.
- [47] Liz-Marzán, L. M. *Langmuir* **2005**, *22*, 32–41.
- [48] Mie, G. *Ann. Phys.* **1908**, *330*, 377–445.
- [49] Zeng, S.; Yu, X.; Law, W.-C.; Zhang, Y.; Hu, R.; Dinh, X.-Q.; Ho, H.-P.; Yong, K.-T. *Sensors and Actuators B: Chemical* **2013**, *176*, 1128–1133.
- [50] Link, S.; El-Sayed, M. A. *J. Phys. Chem. B* **1999**, *103*, 4212–4217.
- [51] Garg, N.; Lee, T. R. *Langmuir* **1998**, *14*, 3815–3819.
- [52] Garg, N.; Carrasquillo-Molina, E.; Lee, T. R. *Langmuir* **2002**, *18*, 2717–2726.
- [53] Chen, S.; Murray, R. W. *Langmuir* **1998**, *15*, 682–689.

- [54] Hofmann, A.; Schmiel, P.; Stein, B.; Graf, C. *Langmuir* **2011**, *27*, 15165–15175.
- [55] Shelley, E. J.; Ryan, D.; Johnson, S. R.; Couillard, M.; Fitzmaurice, D.; Nellist, P. D.; Chen, Y.; Palmer, R. E.; Preece, J. A. *Langmuir* **2002**, *18*, 1791–1795.
- [56] Grimme, S.; Schreiner, P. R. *Angew. Chem.* **2011**, *123*, 12849–12853.
- [57] Wei, L.; Tiznado, H.; Liu, G.; Padmaja, K.; Lindsey, J. S.; Zaera, F.; Bocian, D. F. *J. Phys. Chem. B* **2005**, *109*, 23963–23971.
- [58] Sakata, T.; Maruyama, S.; Ueda, A.; Otsuka, H.; Miyahara, Y. *Langmuir* **2007**, *23*, 2269–2272.
- [59] Zhu, S.-E.; et al. *J. Am. Chem. Soc.* **2013**, *135*, 15794–15800.
- [60] Ie, Y.; Hirose, T.; Yao, A.; Yamada, T.; Takagi, N.; Kawai, M.; Aso, Y. *Phys. Chem. Chem. Phys.* **2009**, *11*, 4949–4951.
- [61] Tian, J.; Ding, Y.-D.; Zhou, T.-Y.; Zhang, K.-D.; Zhao, X.; Wang, H.; Zhang, D.-W.; Liu, Y.; Li, Z.-T. *Chem. Eur. J.* **2014**, *20*, 575–584.
- [62] Rueping, M.; Nachtsheim, B. J. *Beilstein Journal of Organic Chemistry* **2010**, *6*, 6.
- [63] Hutchison, J. A.; Uji-i, H.; Deres, A.; Vosch, T.; Rocha, S.; Müller, S.; Bastian, A. A.; Enderlein, J.; Nourouzi, H.; Li, C.; Herrmann, A.; Müllen, K.; De Schryver, F.; Hofkens, J. *Nat. Nano* **2014**, *9*, 131–136.
- [64] Glaser, C. *Justus Liebigs Ann. Chem.* **1870**, *154*, 137–171.
- [65] Chinchilla, R.; Nájera, C. *Chem. Soc. Rev.* **2011**, *40*, 5084–5121.
- [66] Böhm, V.; Herrmann, W. *Eur. J. Org. Chem.* **2000**, *2000*, 3679–3681.
- [67] Sonogashira, K.; Tohda, Y.; Hagihara, N. *Tetrahedron Letters* **1975**, *16*, 4467–4470.
- [68] Smeyanov, A.; Schmidt, A. *Synthetic Communications* **2013**, *43*, 2809–2816.
- [69] Sander, F.; Peterle, T.; Ballav, N.; Wrochem, F. v.; Zharnikov, M.; Mayor, M. *J. Chem. Phys. C* **2010**, *114*, 4118–4125.
- [70] Horn, M.; Mayr, H. *Chem. Eur. J.* **2010**, *16*, 7469–7477.
- [71] Halterman, R. L.; Pan, X.; Martyn, D. E.; Moore, J. L.; Long, A. T. *J. Org. Chem.* **2007**, *72*, 6454–6458.
- [72] Marvel, C. S.; Kaplan, J. F.; Himel, C. M. *J. Am. Chem. Soc.* **1941**, *63*, 1892–1896.

Erklärung zur wissenschaftlichen Redlichkeit

(beinhaltet Erklärung zu Plagiat und Betrug)

~~Bachelorarbeit~~ / Masterarbeit (nicht Zutreffendes bitte streichen)

Titel der Arbeit (Druckschrift):

Name, Vorname (Druckschrift): _____

Matrikelnummer: _____

Hiermit erkläre ich, dass mir bei der Abfassung dieser Arbeit nur die darin angegebene Hilfe zuteil wurde und dass ich sie nur mit den in der Arbeit angegebenen Hilfsmitteln verfasst habe.

Ich habe sämtliche verwendeten Quellen erwähnt und gemäss anerkannten wissenschaftlichen Regeln zitiert.

Diese Erklärung wird ergänzt durch eine separat abgeschlossene Vereinbarung bezüglich der Veröffentlichung oder öffentlichen Zugänglichkeit dieser Arbeit.

ja nein

Ort, Datum: _____

Unterschrift: _____



Dieses Blatt ist in die Bachelor-, resp. Masterarbeit einzufügen.